Published OnlineFirst June 11, 2014; DOI: 10.1158/1078-0432.CCR-13-1559

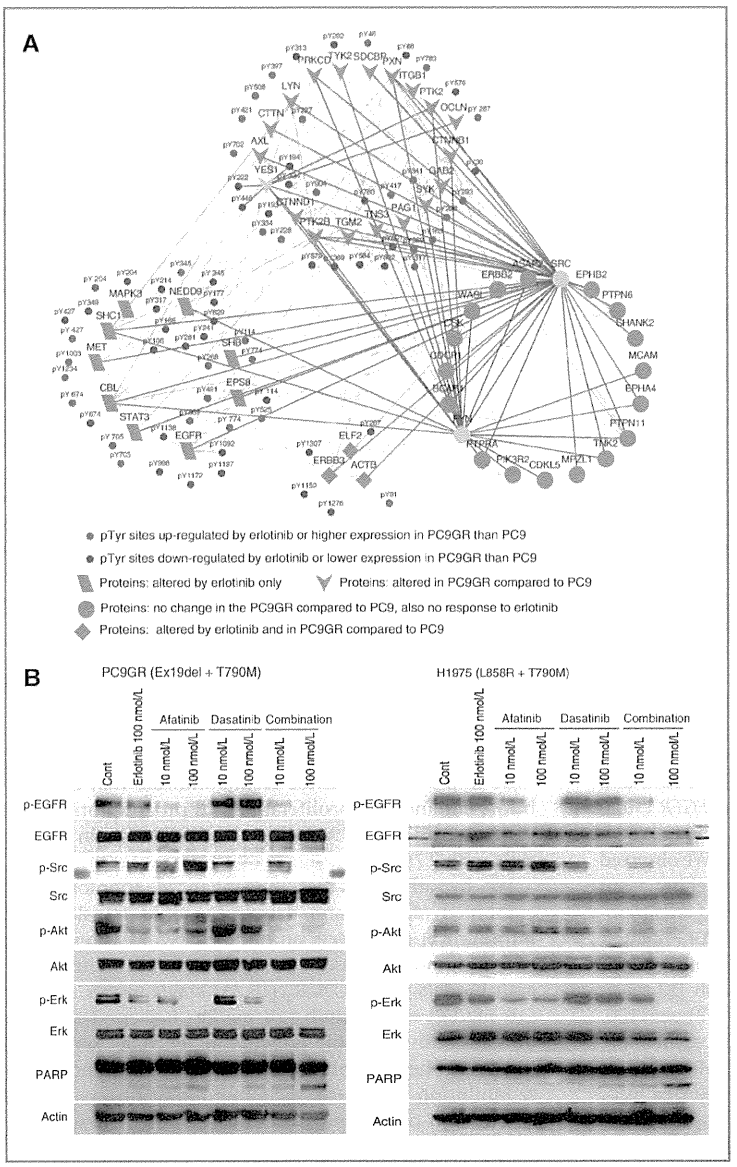

Figure 4. Effects of dasatinib combined with afatinib on EGFR signaling and cell growth in gefitinib-resistant NSCLC cells with T790M. A, pTyr proteins corresponding to pTyr peptides identified in PC9 and PC9GR cells are linked to SFK using InnateDB to capture literature reports and displayed in Cytoscape. Pink circle, pTyr sites upregulated by erlotinib or higher expression in PC9GR than in PC9 cells. Blue circle, pTyr sites downregulated by erlotinib or less expression in PC9GR than in PC9 cells. Yellow circles or V, SFK (SRC, YES1, FYN). Gray circle, pTyr proteins showing no difference between PC9 and PC9GR cells and no change with erlotinib treatment. Gray parallelogram, pTyr proteins altered by erlotinib across PC9 and PC9GR datasets. Gray V, pTyr proteins different between PC9 and PC9GR cells. Gray diamond, pTyr proteins different between PC9 and PC9GR cells and showing changes with erlotinib treatment. B, PC9GR and H1975 cells were incubated for 6 hours (or 24 hours for PARP) in the absence or presence of erlotinib (100 nmol/L), afatinib (10 and 100 nmol/L), dasatinib (10 and 100 nmol/L), or afatinib and dasatinib in combination (10 and 100 nmol/L), as indicated. Cell lysates were subjected to protein expression analysis with antibodies to pEGFR, EGFR, pAkt, Akt, pErk, Erk, pSrc family, Src, or PARP along with antibodies to β-actin as a loading control. (*Continued on the following page.*)

pTyr sites corresponding to 117, 95, 111, and 87 proteins, respectively (Supplementary Table S4). Importantly, 83 unique pTyr sites on 65 proteins identified from mass spectrometry experiments in PC9 cells were also observed active in human patient tissues (Supplementary Fig. S11 and Supplementary Table S5). This included: EGFR (pTyr1172, 1197), MET (pTyr1234), SFKs including SRC (pTyr 419), FYN (pTyr 214, 420), LYN (pTyr 32, 193, 104, 397), YES1 (pTyr223, 426), MK01 (pTyr 187), MK03 (pTyr 204), STAT3 (pTyr 705), and AXL (pTyr 886). These results in human tumor tissues from patients with *EGFR* mutations well validate our findings gained from cell line model, suggesting the potential of clinical application of our findings in this study.

Activation of Src or MET in human lung tumor samples with T790M gatekeeper *EGFR* mutations

To validate that Src phosphorylation is indeed observed as a target in human NSCLC samples with T790M gatekeeper mutation, we examined the expression of phosphorylated Src (Tyr 416) in tumor samples with T790M using immunohistochemical staining. We found pSrc in all *EGFR* T790M-positive tissue specimens, including 2 paired samples of pre- and post-EGFR-TKI treatment, with

Published OnlineFirst June 11, 2014; DOI: 10.1158/1078-0432.CCR-13-1559

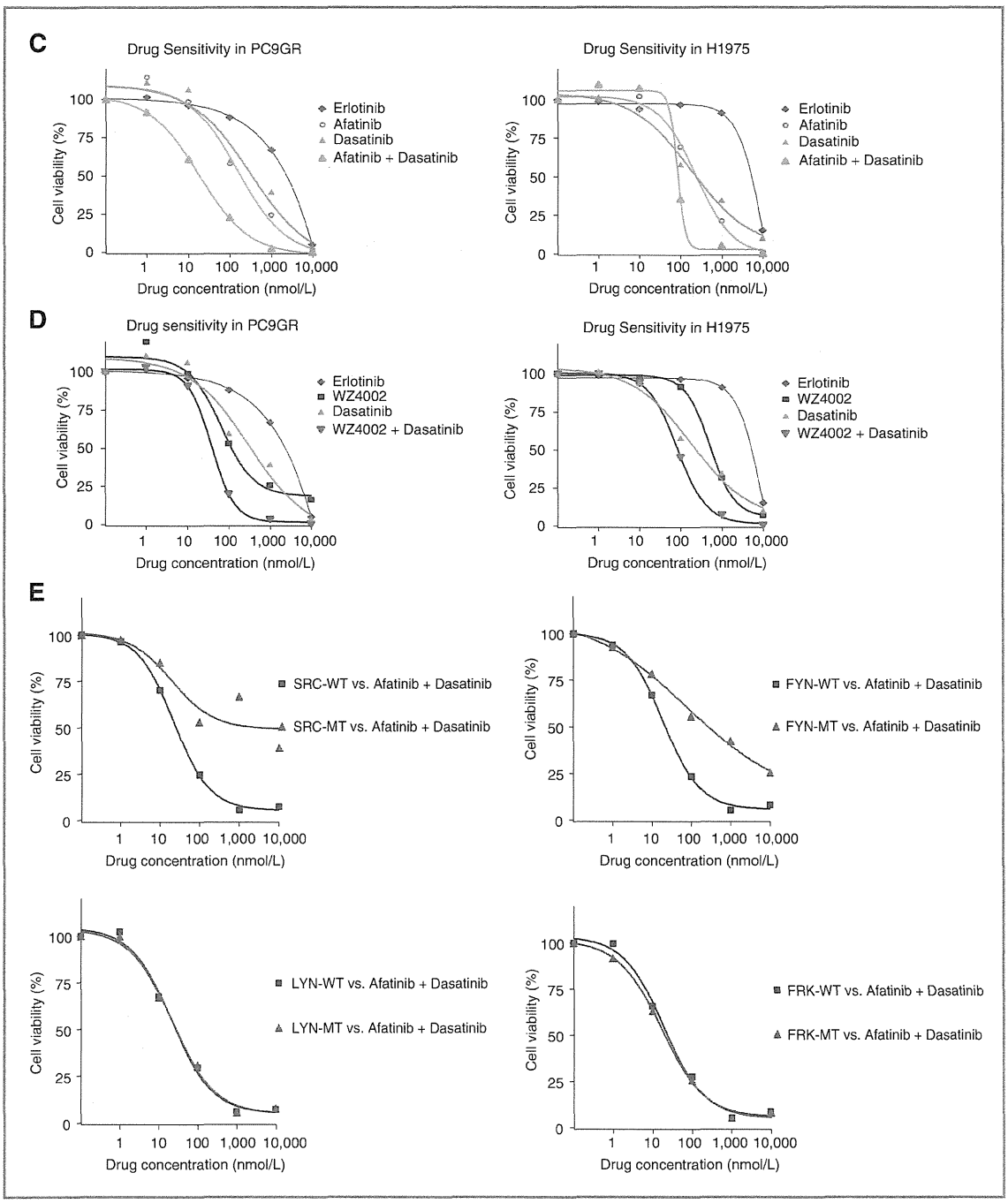

Figure 4. (*Continued.*) C, PC9GR and H1975 cells were treated for 72 hours with increasing concentrations of erlotinib alone, afatinib alone, dasatinib alone, or afatinib + dasatinib. D, PC9GR and H1975 cells were treated for 72 hours with increasing concentrations of erlotinib alone, WZ4002 alone, dasatinib alone, or WZ4002 + dasatinib. Data generated by cell viability assay (CellTiter-Glo) are expressed as a percentage of the value for untreated cells. Determinations were done in triplicate. E, PC9GR cells were infected with lentivirus expressing wild-type and mutant gatekeeper forms of each indicated Src family kinase for 48 hours. Subsequently, cells were exposed to increasing concentrations of afatinib plus dasatinib for 72 hours, after which cell viability was assessed by cell viability assay (CellTiter-Glo). Data are expressed as a percentage of the value for untreated cells. Determinations were done in triplicate. Please view online version for full details.

Published OnlineFirst June 11, 2014; DOI: 10.1158/1078-0432.CCR-13-1559

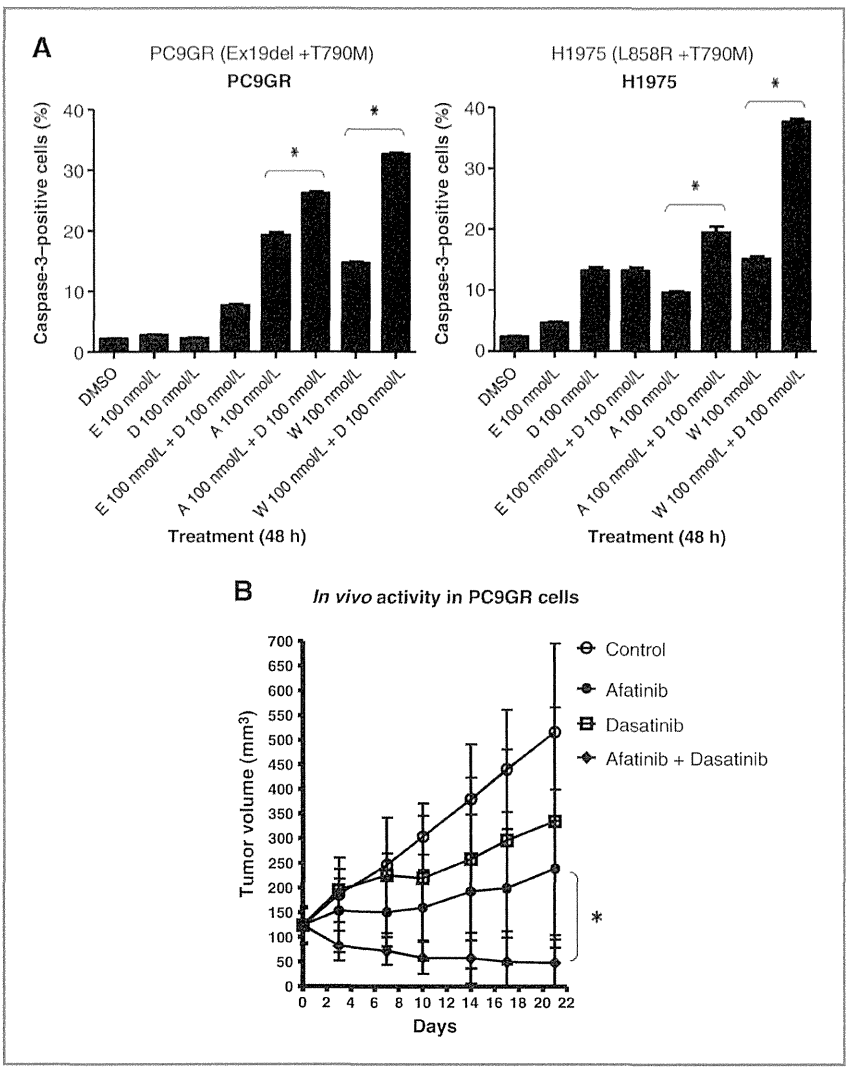

Figure 5. Effects of dasatinib combined with afatinib on apoptosis and *in vivo* tumor regression in gefitinib-resistant NSCLC cells with T790M. A, apoptosis assay was carried out using PE-conjugated caspase-3 antibody, following incubation of PC9GR or H1975 cells for 72 hours with DMSO, erlotinib (E), dasatinib (D), erlotinib + dasatinib, afatinib (A), afatinib + dasatinib, WZ4002 (W), and WZ4002 + dasatinib. Values are expressed as a percentage of caspase-3-positive cells. Determinations were done in triplicate. Bars, SD. *, $P < 0.001$ versus DMSO or each single agent (Student *t* test). B, Nude mice with tumor xenografts established by subcutaneous implantation of PC9GR cells were treated daily for 21 days with vehicle (control), afatinib (10 mg/kg), dasatinib (15 mg/kg), or afatinib + dasatinib by oral gavage. Tumor volume was determined at the indicated times after the onset of treatment. Points, mean of values from 5 mice/group; bars, SE. *, $P < 0.05$ for afatinib combined with dasatinib versus control or each agent alone by ANOVA (Tukey–Kramer comparison). (*Continued on the following page.*)

varied intensities and cellularity (Table 1; Fig. 5C). These results confirmed results from cell lines that Src activity persists in *EGFR* T790M-positive tumor tissues. We further examined changes in tyrosine phosphorylated MET expression in matched pre- and post-EGFR-TKI treatment patient tumor tissue specimens. We found evidence for increased tyrosine phosphorylated MET in one patient (patient 10 in Table 1) that was not due to increased total MET protein (Fig. 5D), whereas no evidence was found in the second patient (patient 9 in Table 1) for which pre- and posttreatment biopsy tissues were available for study. These results provide further support using tumor tissues that MET tyrosine phosphorylation can occur in T790M-containing tissues and this can be independent of total MET expression.

Discussion

We applied tyrosine phosphorylation profiling using LC/MS-MS to directly compare an EGFR-TKI–sensitive cell line versus its acquired resistance counterpart to uncover additional resistance mechanisms and propose cotargeting strategies to enhance the effects of agents specifically targeting the T790M EGFR allele. To our knowledge, this is the first such report to apply a mass spectrometry–based phosphoproteomics approach to compare the molecular networks between EGFR-TKI–sensitive and -resistant pairs. The driving force behind this approach is the limited efficacy of irreversible EGFR-TKIs in targeting T790M, as shown in both preclinical and clinical studies (8, 9, 12, 14–19), and the ability of

Published OnlineFirst June 11, 2014; DOI: 10.1158/1078-0432.CCR-13-1559

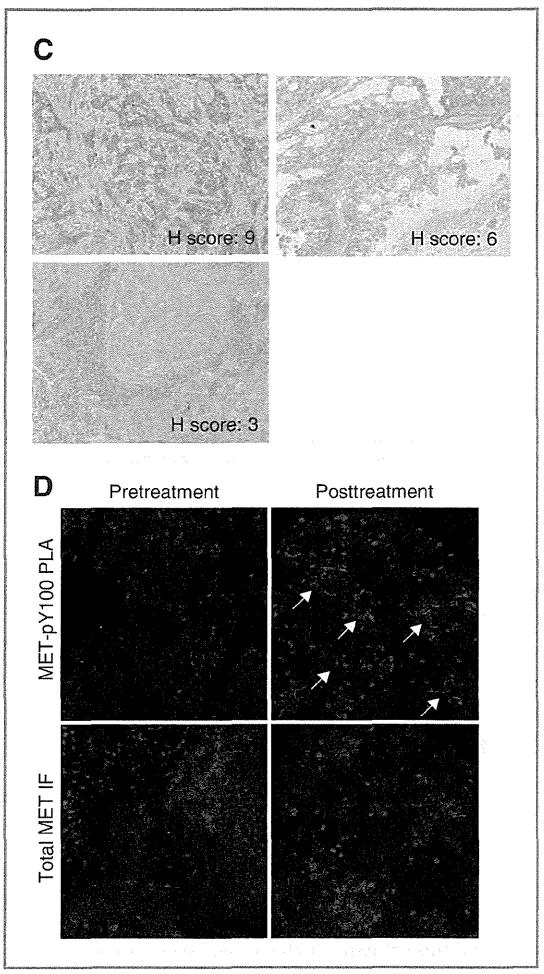

Figure 5. (*Continued.*) C, evidence for activation of Src in the T790M-positive biopsy specimens. Immunohistochemical staining was used to detect expression of tyrosine phosphorylation Src (Tyr416) in 10 EGFR T790M-positive tissue specimens. H score (intensity × cellularity) was calculated for each sample, with scores 0 and 9 representing the lowest and highest expression, respectively. Three representative ×200 images show the different levels of pSrc expression in EGFR T790M-positive human lung specimen. D, evidence for increased MET tyrosine phosphorylation in posttreatment T790M biopsy specimens. Proximity ligation assays (PLA) for MET and pY100 were performed to assess MET phosphorylation in serial biopsy specimens obtained from an adenocarcinoma patient (right lung, lower lobe, 33 months apart). Original biopsy confirmed *EGFR* exon21 L858R mutation; rebiopsy confirmed L858R/T790M mutation. Top, evidence of MET-pY PLA signal in pretreatment biopsy, while clusters of highly phosphorylated MET are observed in the posttreatment biopsy. MET-pY PLA was localized to cytokeratin (+)-staining regions (data not shown). Bottom, increased MET-pY PLA signal is not due to increased total MET protein.

other tyrosine kinases, especially RTKs, to limit EGFR-TKI efficacy. Through a systematic interrogation of pTyr peptides and proteins using LC/MS-MS, we identified both RTKs and non-RTKs able to be recruited to confer erlotinib sensitivity. In PC9GR cells, we identified higher levels of pTyr peptides corresponding to MET signaling, including more MET, ROR1, and Gab1/2 proteins. Interestingly, this coordinated activation of MET signaling was not secondary to *MET* gene amplification, as our FISH results revealed no amplification of the *MET* gene. The results with the basal phosphoproteome corresponded to HGF's strong effects in protecting both PC9 and PC9GR cells from erlotinib or afatinib, respectively. In addition, these results suggest a form of "lineage" addiction, whereby resistant cells with T790M can carry forward RTKs that can cooperate to drive resistance. Importantly, these results suggest that interrogating protein activation status or network signaling may highlight proteins that play a role in protecting cells against EGFR-TKI, especially when in a microenvironment rich with cognate growth factor ligands. Despite observing more AXL pTyr peptides in PC9GR cells, we demonstrated no ability of AXL pathway activation by Gas6 ligand to drive resistance to either erlotinib or afatinib. The reasons for this are not clear, but one limit of our approach was the lack of absolute measurements of pTyr peptides. It is possible that, compared with MET or IRS2 pTyr peptides, pTyr peptides corresponding to AXL are far lower in absolute amount and thus are inefficient to compete for downstream signaling effectors. It will be interesting and important to determine how basal phosphoproteome measurements can predict the effects of growth factor protection against targeted agents. As AXL signaling still remains poorly understood, another explanation for our results could be the limited or absence of key adaptors or other effector proteins involved in AXL signaling.

Using pTyr peptide data obtained from both PC9 and PC9GR cells exposed to erlotinib, we identified proteins downstream of EGFR in these cells with mutant gain-of-function EGFR proteins. One of the more interesting findings was that nearly half of the statistically significant pTyr peptides were increased in abundance following erlotinib treatment. It is increasingly recognized that signaling pathways display large amounts of crosstalk and that adaptive resistance mechanisms have been observed in cells exposed to targeted agents (41). Our results match our investigations using purified Src homology-2 domains to profile tyrosine kinase signaling in lung cancer cells, where we observed increased pTyr signaling in multiple lung cancer cells exposed to TKIs (42). Similar events have also been observed in crizotinib-treated EML4-ALK cells and dasatinib-treated DDR2-mutant lung cancer cells, arguing that these paradoxical changes are consistent across multiple tumor types and kinase inhibitors (unpublished observations). The underlying mechanisms of these changes require additional study, as they could be important in promoting adaptive resistance to targeted agents and could in some cases cooperate with microenvironmental factors, such as growth factors, to limit TKI efficacy. Collectively, these results suggest that cell intrinsic (receptors, signaling proteins) and extrinsic (ligands) factors can collaborate

Published OnlineFirst June 11, 2014; DOI: 10.1158/1078-0432.CCR-13-1559

Table 1. Src phosphorylation detected in human NSCLC samples with T790M gatekeeper mutation

Patient ID	EGFR mutant	H score	Intensity	Cellularity
1	T790M/L858R	3	1	3
2	T790M/19del(E746-A750)	4	2	2
3	T790M/19del(E746-A750)	6	2	3
4	T790M/L858R	6	2	3
5	T790M/19del(E746-A750)	6	2	3
6	T790M/19del(E746-A750)	9	3	3
7	T790M/19del(E746-A750)	9	3	3
8	T790M/L858R	9	3	3
9 (Pre-TKI)	19del(E746-A750)	9	3	3
9 (Post-TKI)	T790M/19del(E746-A750)	9	3	3
10 (Pre-TKI)	L858R	4	2	2
10 (Post-TKI)	T790M/L858R	9	3	3

NOTE: Patient 9 was treated with "gefitinib and erlotinib." Patient 10 was treated with "gefitinib and erlotinib + ARQ197 (MET-TKI)."

to drive resistance to kinase inhibitors in a systems-level manner.

Our phosphoproteomics analyses in PC9 and PC9GR cells demonstrated that SFKs are also critical as an EGFR-independent cosignal in NSCLC cells with T790M. These results were enabled by tyrosine phosphorylation profiling combined with analysis of proteins based on known protein–protein interactions. We validated the inferences derived from the phosphoproteomics by showing that afatinib combined with dasatinib resulted in antitumor activity regarding cell proliferation and apoptosis in PC9GR, H1975, HCC4006-T790M, and HCC827-T790M cells (each harboring T790M). These results appear to be generalized to additional T790M EGFR-TKIs, as dasatinib demonstrated similar combination effects with the T790M-selective EGFR-TKI WZ4002 (40). We did not observe combination effects with afatinib plus dasatinib compared with either agent alone in cells with TKI-sensitive *EGFR* mutation only (PC9, HCC4006, and HCC827 cells) or wild-type *EGFR* (H460, A549, and H1299 cells). The enhanced apoptosis with combined afatinib and dasatinib in the cells with T790M translated into improved *in vivo* effects on tumor growth in PC9GR cells. Collectively, our results suggest that dasatinib can be generally used as a combination therapy with irreversible or T790M-selective EGFR-TKIs for patients with NSCLC who acquired EGFR-TKI resistance associated with T790M.

As our approach was limited to examining the tyrosine phosphoproteome, we were unable to detect serine/threonine signaling including mTOR/AKT or MEK/Erk pathways both of which are also essential for carcinogenesis. Previous studies have indicated that mTOR inhibitor combined with MEK inhibitor or irreversible EGFR-TKI is potential strategy to overcome T790M (21, 43). Further studies examining the global phosphoproteome, such as with immobilized metal affinity chromatography which can detect serine/threonine phosphopeptides (44), could identify other proteins and pathways that may play roles in EGFR TKI resistance.

Although single-agent dasatinib has no activity in patients with NSCLC with TKI-sensitive *EGFR* mutation who acquired resistance to EGFR-TKI (45), our results suggest a role for SFKs in maintaining downstream signaling despite irreversible EGFR-TKIs and support further studies of irreversible EGFR-TKIs combined with dasatinib in patients with NSCLC who acquire resistance to EGFR-TKI. Src is known to be both an upstream activator and a downstream mediator of EGFR, and its phosphorylation is detected in about one-third of lung cancer tumors (46, 47). Although MET activation might not be always observed in the presence of T790M based on our *in vitro* and tumor tissue analysis, pSrc seems to be generally detected in our NSCLC tumor samples harboring T790M, consistent with our results of cell models. In addition, our mass spectrometry data from tumor samples with TKI-sensitive *EGFR* mutation demonstrated a high degree of overlap with results from cell models, thereby validating the overall approach. These results from tumor samples suggest that our results from lung cancer cell line models are applicable to translate in to the clinic. Our previous chemical and phosphoproteomic characterization identified nearly 40 different kinase targets of dasatinib and showed that SRC, FYN, and EGFR are relevant targets for dasatinib action in NSCLC (32). Our recent phase I/II study showed that dasatinib combined with erlotinib is tolerable, with 63% of patients with advanced NSCLC showing disease control, including two having partial response and one having bone response (48). Another group also showed that dasatinib combined with erlotinib is safe and feasible in NSCLC (49).

On the basis of these clinical studies along with the experiments reported here, dasatinib has potential clinical activity in NSCLC treatment, but this is limited to

Published OnlineFirst June 11, 2014; DOI: 10.1158/1078-0432.CCR-13-1559

combinations with T790M-targeted agents and in genotype-specific patients. This will be formally tested in a phase I trial of afatinib and dasatinib (NCT01999985). Our results also highlight the ability of phosphoproteomics to identify other important mediators of drug sensitivity, and examination of these proteins may be important in clinical studies of T790M-targeting agents.

Disclosure of Potential Conflicts of Interest

E.B. Haura reports receiving a commercial research grant from Boehringer-Ingelheim. No potential conflicts of interest were disclosed by the other authors.

Authors' Contributions

Conception and design: T. Yoshida, G. Zhang, E.B. Haura
Development of methodology: T. Yoshida, G. Zhang, M.A. Smith, A.S. Lopez, Y. Bai, J. Koomen, E.B. Haura
Acquisition of data (provided animals, acquired and managed patients, provided facilities, etc.): T. Yoshida, G. Zhang, M.A. Smith, B. Fang, J. Koomen, K. Nakagawa, E.B. Haura
Analysis and interpretation of data (e.g., statistical analysis, biostatistics, computational analysis): G. Zhang, M.A. Smith, A.S. Lopez, Y. Bai, B. Fang, B. Rawal, K.J. Fisher, A.Y. Chen, I. Okamoto, K. Nakagawa, E.B. Haura
Writing, review, and/or revision of the manuscript: T. Yoshida, G. Zhang, M.A. Smith, B. Fang, J. Koomen, B. Rawal, A.Y. Chen, K. Nakagawa, E.B. Haura
Administrative, technical, or material support (i.e., reporting or organizing data, constructing databases): T. Yoshida, G. Zhang, M.A. Smith, A.S. Lopez, Y. Bai, J. Li, M. Kitano, Y. Morita, H. Yamaguchi, K. Shibata, T. Okabe, I. Okamoto, K. Nakagawa, E.B. Haura
Study supervision: K. Nakagawa, E.B. Haura

Acknowledgments

The authors thank the Moffitt pY Group, the Kinki University Medical Oncology Research Group, Tsutomu Iwasa, and Kunio Okamoto for helpful discussions, Rasa Hamilton for editorial assistance, Fumi Kinose for assistance with cell culture, and Linda Ley and Carol Ulge for administrative assistance. The authors also thank BML, Inc and SRL, Inc for technical assistance.

Grant Support

The work was partially funded by grants from the Moffitt Cancer Center SPORE in Lung Cancer (P50-CA119997), the V Foundation for Cancer Research, and in part by the National Cancer Institute, part of the NIH, through grant number 2 P30-CA76292-14, which provide support to the Proteomics Core, the Flow Cytometry Core, the Tissue Core, and the Animal Facility at the H. Lee Moffitt Cancer Center and Research Institute, an NCI-designated Comprehensive Cancer Center.

The costs of publication of this article were defrayed in part by the payment of page charges. This article must therefore be hereby marked *advertisement* in accordance with 18 U.S.C. Section 1734 solely to indicate this fact.

Received June 13, 2013; revised April 9, 2014; accepted April 23, 2014; published OnlineFirst June 11, 2014.

References

1. Mok TS, Wu YL, Thongprasert S, Yang CH, Chu DT, Saijo N, et al. Gefitinib or carboplatin-paclitaxel in pulmonary adenocarcinoma. N Engl J Med 2009;361:947–57.
2. Mitsudomi T, Morita S, Yatabe Y, Negoro S, Okamoto I, Tsurutani J, et al. Gefitinib versus cisplatin plus docetaxel in patients with non-small-cell lung cancer harbouring mutations of the epidermal growth factor receptor (WJTOG3405): an open label, randomised phase 3 trial. Lancet Oncol 2010;11:121–8.
3. Kobayashi S, Boggon TJ, Dayaram T, Janne PA, Kocher O, Meyerson M, et al. EGFR mutation and resistance of non-small-cell lung cancer to gefitinib. N Engl J Med 2005;352:786–92.
4. Pao W, Miller VA, Politi KA, Riely GJ, Somwar R, Zakowski MF, et al. Acquired resistance of lung adenocarcinomas to gefitinib or erlotinib is associated with a second mutation in the EGFR kinase domain. PLoS Med 2005;2:e73.
5. Kosaka T, Yatabe Y, Endoh H, Yoshida K, Hida T, Tsuboi M, et al. Analysis of epidermal growth factor receptor gene mutation in patients with non-small cell lung cancer and acquired resistance to gefitinib. Clin Cancer Res 2006;12:5764–9.
6. Sequist LV, Waltman BA, Dias-Santagata D, Digumarthy S, Turke AB, Fidias P, et al. Genotypic and histological evolution of lung cancers acquiring resistance to EGFR inhibitors. Sci Transl Med 2011;3:75ra26.
7. Yu HA, Arcila ME, Rekhtman N, Sima CS, Zakowski MF, Pao W, et al. Analysis of tumor specimens at the time of acquired resistance to EGFR-TKI therapy in 155 patients with EGFR-mutant lung cancers. Clin Cancer Res 2013;19:2240–7.
8. Engelman JA, Mukohara T, Zejnullahu K, Lifshits E, Borras AM, Gale CM, et al. Allelic dilution obscures detection of a biologically significant resistance mutation in EGFR-amplified lung cancer. J Clin Invest 2006;116:2695–706.
9. Engelman JA, Zejnullahu K, Gale CM, Lifshits E, Gonzales AJ, Shimamura T, et al. PF00299804, an irreversible pan-ERBB inhibitor, is effective in lung cancer models with EGFR and ERBB2 mutations that are resistant to gefitinib. Cancer Res 2007;67:11924–32.
10. Li D, Ambrogio L, Shimamura T, Kubo S, Takahashi M, Chirieac LR, et al. BIBW2992, an irreversible EGFR/HER2 inhibitor highly effective in preclinical lung cancer models. Oncogene 2008;27:4702–11.
11. Kwak EL, Sordella R, Bell DW, Godin-Heymann N, Okimoto RA, Brannigan BW, et al. Irreversible inhibitors of the EGF receptor may circumvent acquired resistance to gefitinib. Proc Natl Acad Sci U S A 2005;102:7665–70.
12. Sos ML, Rode HB, Heynck S, Peifer M, Fischer F, Kluter S, et al. Chemogenomic profiling provides insights into the limited activity of irreversible EGFR inhibitors in tumor cells expressing the T790M EGFR resistance mutation. Cancer Res 2010;70:868–74.
13. Yun CH, Mengwasser KE, Toms AV, Woo MS, Greulich H, Wong KK, et al. The T790M mutation in EGFR kinase causes drug resistance by increasing the affinity for ATP. Proc Natl Acad Sci U S A 2008;105:2070–5.
14. Yu Z, Boggon TJ, Kobayashi S, Jin C, Ma PC, Dowlati A, et al. Resistance to an irreversible epidermal growth factor receptor (EGFR) inhibitor in EGFR-mutant lung cancer reveals novel treatment strategies. Cancer Res 2007;67:10417–27.
15. Godin-Heymann N, Ulkus L, Brannigan BW, McDermott U, Lamb J, Maheswaran S, et al. The T790M "gatekeeper" mutation in EGFR mediates resistance to low concentrations of an irreversible EGFR inhibitor. Mol Cancer Ther 2008;7:874–9.
16. Shimamura T, Li D, Ji H, Haringsma HJ, Liniker E, Borgman CL, et al. Hsp90 inhibition suppresses mutant EGFR-T790M signaling and overcomes kinase inhibitor resistance. Cancer Res 2008;68:5827–38.
17. Yamada T, Matsumoto K, Wang W, Li Q, Nishioka Y, Sekido Y, et al. Hepatocyte growth factor reduces susceptibility to an irreversible epidermal growth factor receptor inhibitor in EGFR-T790M mutant lung cancer. Clin Cancer Res 2010;16:174–83.
18. Ercan D, Zejnullahu K, Yonesaka K, Xiao Y, Capelletti M, Rogers A, et al. Amplification of EGFR T790M causes resistance to an irreversible EGFR inhibitor. Oncogene 2010;29:2346–56.
19. Miller VA, Hirsh V, Cadranel J, Chen YM, Park K, Kim SW, et al. Afatinib versus placebo for patients with advanced, metastatic non-small-cell lung cancer after failure of erlotinib, gefitinib, or both, and one or two lines of chemotherapy (LUX-Lung 1): a phase 2b/3 randomised trial. Lancet Oncol 2012;13:528–38.
20. Regales L, Gong Y, Shen R, de Stanchina E, Vivanco I, Goel A, et al. Dual targeting of EGFR can overcome a major drug resistance

Published OnlineFirst June 11, 2014; DOI: 10.1158/1078-0432.CCR-13-1559

mutation in mouse models of EGFR mutant lung cancer. J Clin Invest 2009;119:3000–10.
21. Li D, Shimamura T, Ji H, Chen L, Haringsma HJ, McNamara K, et al. Bronchial and peripheral murine lung carcinomas induced by T790M-L858R mutant EGFR respond to HKI-272 and rapamycin combination therapy. Cancer Cell 2007;12:81–93.
22. Stommel JM, Kimmelman AC, Ying H, Nabioullin R, Ponugoti AH, Wiedemeyer R, et al. Coactivation of receptor tyrosine kinases affects the response of tumor cells to targeted therapies. Science 2007;318:287–90.
23. Wilson TR, Fridlyand J, Yan Y, Penuel E, Burton L, Chan E, et al. Widespread potential for growth-factor-driven resistance to anticancer kinase inhibitors. Nature 2012;487:505–9.
24. Harbinski F, Craig VJ, Sanghavi S, Jeffery D, Liu L, Sheppard KA, et al. Rescue screens with secreted proteins reveal compensatory potential of receptor tyrosine kinases in driving cancer growth. Cancer Discov 2012;2:948–59.
25. Yano S, Wang W, Li Q, Matsumoto K, Sakurama H, Nakamura T, et al. Hepatocyte growth factor induces gefitinib resistance of lung adenocarcinoma with epidermal growth factor receptor-activating mutations. Cancer Res 2008;68:9479–87.
26. Machida K, Eschrich S, Li J, Bai Y, Koomen J, Mayer BJ, et al. Characterizing tyrosine phosphorylation signaling in lung cancer using SH2 profiling. PLoS ONE 2010;5:e13470.
27. Naoki K, Soejima K, Okamoto H, Hamamoto J, Hida N, Nakachi I, et al. The PCR-invader method (structure-specific 5′ nuclease-based method), a sensitive method for detecting EGFR gene mutations in lung cancer specimens; comparison with direct sequencing. Int J Clin Oncol 2011;16:335–44.
28. Engelman JA, Zejnullahu K, Mitsudomi T, Song Y, Hyland C, Park JO, et al. MET amplification leads to gefitinib resistance in lung cancer by activating ERBB3 signaling. Science 2007;316:1039–43.
29. Zhang G, Fang B, Liu RZ, Lin H, Kinose F, Bai Y, et al. Mass spectrometry mapping of epidermal growth factor receptor phosphorylation related to oncogenic mutations and tyrosine kinase inhibitor sensitivity. J Proteome Res 2011;10:305–19.
30. Lynn DJ, Winsor GL, Chan C, Richard N, Laird MR, Barsky A, et al. InnateDB: facilitating systems-level analyses of the mammalian innate immune response. Mol Syst Biol 2008;4:218.
31. Saito R, Smoot ME, Ono K, Ruscheinski J, Wang PL, Lotia S, et al. A travel guide to Cytoscape plugins. Nat Methods 2012;9:1069–76.
32. Li J, Rix U, Fang B, Bai Y, Edwards A, Colinge J, et al. A chemical and phosphoproteomic characterization of dasatinib action in lung cancer. Nat Chem Biol 2010;6:291–9.
33. Ogino A, Kitao H, Hirano S, Uchida A, Ishiai M, Kozuki T, et al. Emergence of epidermal growth factor receptor T790M mutation during chronic exposure to gefitinib in a non small cell lung cancer cell line. Cancer Res 2007;67:7807–14.
34. Rush J, Moritz A, Lee KA, Guo A, Goss VL, Spek EJ, et al. Immunoaffinity profiling of tyrosine phosphorylation in cancer cells. Nat Biotechnol 2005;23:94–101.
35. Gentile A, Lazzari L, Benvenuti S, Trusolino L, Comoglio PM. Ror1 is a pseudokinase that is crucial for Met-driven tumorigenesis. Cancer Res 2011;71:3132–41.
36. Zhang Z, Lee JC, Lin L, Olivas V, Au V, LaFramboise T, et al. Activation of the AXL kinase causes resistance to EGFR-targeted therapy in lung cancer. Nat Genet 2012;44:852–60.
37. Komiyama NH, Watabe AM, Carlisle HJ, Porter K, Charlesworth P, Monti J, et al. SynGAP regulates ERK/MAPK signaling, synaptic plasticity, and learning in the complex with postsynaptic density 95 and NMDA receptor. J Neurosci 2002;22:9721–32.
38. Rumbaugh G, Adams JP, Kim JH, Huganir RL. SynGAP regulates synaptic strength and mitogen-activated protein kinases in cultured neurons. Proc Natl Acad Sci U S A 2006;103:4344–51.
39. Cantalupo G, Alifano P, Roberti V, Bruni CB, Bucci C. Rab-interacting lysosomal protein (RILP): the Rab7 effector required for transport to lysosomes. EMBO J 2001;20:683–93.
40. Zhou W, Ercan D, Chen L, Yun CH, Li D, Capelletti M, et al. Novel mutant-selective EGFR kinase inhibitors against EGFR T790M. Nature 2009;462:1070–4.
41. Chandarlapaty S. Negative feedback and adaptive resistance to the targeted therapy of cancer. Cancer Discov 2012;2:311–9.
42. Machida K, Thompson CM, Dierck K, Jablonowski K, Karkkainen S, Liu B, et al. High-throughput phosphotyrosine profiling using SH2 domains. Mol Cell 2007;26:899–915.
43. Faber AC, Li D, Song Y, Liang MC, Yeap BY, Bronson RT, et al. Differential induction of apoptosis in HER2 and EGFR addicted cancers following PI3K inhibition. Proc Natl Acad Sci U S A 2009;106:19503–8.
44. Kim JY, Welsh EA, Oguz U, Fang B, Bai Y, Kinose F, et al. Dissection of TBK1 signaling via phosphoproteomics in lung cancer cells. Proc Natl Acad Sci U S A 2013;110:12414–9.
45. Johnson ML, Riely GJ, Rizvi NA, Azzoli CG, Kris MG, Sima CS, et al. Phase II trial of dasatinib for patients with acquired resistance to treatment with the epidermal growth factor receptor tyrosine kinase inhibitors erlotinib or gefitinib. J Thorac Oncol 2011;6:1128–31.
46. Zhang J, Kalyankrishna S, Wislez M, Thilaganathan N, Saigal B, Wei W, et al. SRC-family kinases are activated in non-small cell lung cancer and promote the survival of epidermal growth factor receptor-dependent cell lines. Am J Pathol 2007;170:366–76.
47. Leung EL, Tam IY, Tin VP, Chua DT, Sihoe AD, Cheng LC, et al. SRC promotes survival and invasion of lung cancers with epidermal growth factor receptor abnormalities and is a potential candidate for molecular-targeted therapy. Mol Cancer Res 2009;7:923–32.
48. Haura EB, Tanvetyanon T, Chiappori A, Williams C, Simon G, Antonia S, et al. Phase I/II study of the Src inhibitor dasatinib in combination with erlotinib in advanced non-small-cell lung cancer. J Clin Oncol 2010;28:1387–94.
49. Johnson FM, Tang X, Tran HT, McIntyre C, Price J, Lee JJ, et al. A phase I/II study combining dasatinib (D) and erlotinib (E) in non-small cell lung cancer. J Clin Oncol 31, 2013 (suppl; abstr 8102).

Breast Cancer Res Treat
DOI 10.1007/s10549-014-3121-5

PRECLINICAL STUDY

Transcriptional *CCND1* expression as a predictor of poor response to neoadjuvant chemotherapy with trastuzumab in HER2-positive/ER-positive breast cancer

M. Tanioka · K. Sakai · T. Sudo · T. Sakuma · K. Kajimoto · K. Hirokaga · S. Takao · S. Negoro · H. Minami · K. Nakagawa · K. Nishio

Received: 27 June 2014 / Accepted: 30 August 2014

Abstract Several trials have confirmed that the pathological complete response (pCR) rates after neoadjuvant chemotherapy (NAC) are significantly lower in HER2-positive/ER-positive patients than in HER2-positive/ER-negative patients. To understand this phenomenon, we investigated the association between NAC resistance and *CCND1*, which is frequently overexpressed in ER-positive tumors. Pretreatment formalin-fixed tumor tissues were collected from 75 HER2-positive patients receiving NAC comprised anthracyclines, taxanes, and trastuzumab. Seventeen gene transcripts along with PIK3CA mutations were detected using MassARRAY (Sequenom, San Diego, CA). The gene expression levels were dichotomized according to the median values. The immunohistochemical expression of ER, PTEN, BCL-2, and cyclin D1 was scored. The relationship between the variables was assessed using the Spearman correlation. A logistic regression analysis was performed to detect predictors of pCR, which was defined as no invasive tumor in the breast or axilla. Forty-seven percent of the cases were ER-positive and 52 % (40/63 % in ER-positive/ER-negative) achieved a pCR. Among the ER-positive patients, the *CCND1* gene expression level was 2.1 times higher than that in ER-negative patients and was significantly correlated with the expression of cyclin D1 protein. In a univariate analysis, a pCR was associated with high mRNA levels of *ESR1, PGR, LMTK3, HER2, IGF1R, INPP4B, PDL-1, BCL-2*, and *CCND1* ($P \leq 0.05$). In contrast, none of these genes were significantly correlated with a pCR among the ER-negative tumors and only *EGFR* was significantly correlated with a pCR. PIK3CA mutations or PTEN loss were not associated with a pCR in either group. After excluding *ESR1* ($r = 0.58$), *PGR* ($r = 0.64$), and *IGF1R* ($r = 0.59$), the expressions of which were correlated with *CCND1*, a multivariate analysis revealed that *CCND1* [$P = 0.043$; OR, 0.16] and *HER2* [$P = 0.012$; OR, 11.2] retained its predictive value for pCR among ER-positive patients, but not among ER-negative patients. A High Level of *CCND1* gene expression is a poor predictor of a pCR and provides a rationale for evaluating CDK4/6 inhibitors in HER2-positive/ER-positive breast cancer patients.

Keywords *CCND1* · cyclin D1 · HER2 · ER · Pathological complete response · MassARRAY

M. Tanioka (✉) · S. Negoro
Department of Medical Oncology, Hyogo Cancer Center, 13-70 Kitaoji-cho, Akashi, Hyogo 673-8558, Japan
e-mail: makitanioka123456@yahoo.co.jp

M. Tanioka · H. Minami
Medical Oncology/Hematology, Kobe University Graduate School of Medicine, Kobe, Japan

K. Sakai · K. Nishio
Department of Genome Biology, Kinki University Faculty of Medicine, Osaka, Japan

T. Sudo
Section of Translational Research, Hyogo Cancer Center, 13-70 Kitaoji-cho, Akashi, Hyogo 673-8558, Japan

T. Sakuma · K. Kajimoto
Pathology Division, Hyogo Cancer Center, 13-70 Kitaoji-cho, Akashi, Hyogo 673-8558, Japan

K. Hirokaga · S. Takao
Breast Surgery, Hyogo Cancer Center, 13-70 Kitaoji-cho, Akashi, Hyogo 673-8558, Japan

K. Nakagawa
Department of Medical Oncology, Kinki University Faculty of Medicine, Osaka, Japan

Introduction

A pathological complete response (pCR) after neoadjuvant chemotherapy (NAC) predicted the long-term outcome in

Published online: 09 September 2014

two meta-analyses [1, 2]. In human epidermal growth factor receptor 2 (HER2)-overexpressing breast cancer, the addition of trastuzumab to chemotherapy resulted in a pCR rate nearly twice that compared with chemotherapy alone [2]. However, even after NAC with trastuzumab, several trials [3–5] and a meta-analysis [2] have shown that pCR rates are consistently and significantly 12–20 % lower in HER2-positive/ER-positive patients than in HER2-positive/ER-negative patients. In the Translational Breast Cancer Research Consortium 006 (TBCRC 006) trial [6], neoadjuvant lapatinib and trastuzumab with hormonal therapy and without chemotherapy in HER2-positive/ER-positive breast cancer patients yielded a pCR rate of 21 %. Although this study indicated the importance of blocking both HER2 and ER, predictive biomarkers or new agents to combat the endocrine resistance resulting from the relatively low pCR rate are still needed.

Crosstalk between ER and growth factor receptors such as HER3 [7, 8], IGF1R [7], EGFR [8, 9], and FGFR1 [10] has been implicated as part of this resistance mechanism, and Bcl-2 [11], SRC-1 [12], FOXA1 [13], LMTK3 [14], and cyclin D1 [15] have been identified as ER regulators. Moreover, several PI3 K pathway genes are related to trastuzumab resistance, including PIK3CA mutations [16, 17], PTEN [17], INPP4B [18], and DUSP4 [19]. Therefore, in HER2-positive patients receiving NAC with trastuzumab, the precise mechanism and promising molecular targets of endocrine resistance remain unclear.

Cyclin D1 is a key mediator of cell cycle progression that is overexpressed in approximately 50 % of breast cancer specimens with the corresponding *CCND1* gene amplified in 15 % [20]. Cyclin D1, which has been shown to bind and activate ER [15], binds to cyclin-dependent kinase CDK4/6 [21, 22] and activates CDK4 [23], therefore, it could be a potential molecular biomarker of CDK4/6 inhibitors including palbociclib, which has received a breakthrough therapy designation for ER-positive breast cancer from the Food and Drug Administration (FDA).

Based on this background information, we conducted a hypothesis-generating study using MassARRAY analyses of 17 gene transcripts mentioned above and PIK3CA mutations in addition to immunohistochemical analyses to investigate the predictive value of *CCND1* in resistance to NAC with trastuzumab for patients with HER2-overexpressing breast cancer.

Patients and methods

Patients

Formalin-fixed paraffin-embedded (FFPE) pretreatment biopsy tissues were collected from 75 subjects diagnosed as having stage I–III HER2-positive breast cancer at the Hyogo Cancer Center between 2006 and 2013. All the patients received neoadjuvant chemotherapy with FEC (5-FU [500 mg/m^2], epirubicin [100 mg/m^2], and cyclophosphamide [500 mg/m^2]) every 3 weeks for four cycles followed by trastuzumab and taxane (paclitaxel or docetaxel) and subsequent surgery. The weekly paclitaxel plus trastuzumab regimen consisted of the weekly administration of paclitaxel (80 mg/m^2) and trastuzumab (at a loading dose of 4 mg/kg, followed by 2 mg/kg) for 12 cycles. The triweekly docetaxel plus trastuzumab regimen consisted of the triweekly administration of docetaxel (75 mg/m^2) and trastuzumab (at a loading dose of 8 mg/kg, followed by 6 mg/kg) for four cycles. Tissues were obtained under written general consent for discarded tissues, and the present study was approved by the institutional review board at the Hyogo Cancer Center and Kinki University Hospital. pCR was defined as no invasive tumor in the breast or axilla.

Tissue macrodissection, DNA, and RNA isolation

Five-micrometer-thick sections were prepared and stained with hematoxylin and eosin (H&E). Nine additional sections with a 5-μm thickness were cut, mounted onto glass slides, and used for macrodissection. Tumor areas corresponding to the sampled H&E-stained section were scraped off with a disposable scalpel to ensure a minimum of 70 % of the tumor cells. The samples were collected into plastic tubes.

DNA and RNA were prepared using the AllPrepDNA/RNA FFPE kit (Qiagen, Valencia, CA). DNA/RNA quality and quantity were determined using NanoDrop spectrophotometry (NanoDrop Technologies, Wilmington, DE). RNA was reverse transcribed to produce cDNA.

Quantitative gene expression analysis

The gene expression levels were assayed for 75 tumor samples using the MassARRAY system (Sequenom, San Diego, CA) [24, 25]. The MassARRAY technology involves a three-step process composed of real-time competitive PCR, primer extension, and matrix-assisted laser desorption/ionization time-of-flight (MALDI-TOF) mass spectrometry separation of products on a matrix-loaded silicon chip array to detect several initial molecules.

For the competitive RT-PCR, all the assays and their competitive template (90–110 bp) at known quantities were plexed into a single reaction mix, using the Sequenom iPLEX mass spectrometry platform. Six reactions for each individual cDNA species were performed using six serial dilutions of the competitor, ranging from 10^{-18} to 10^{-13} M. In this manner, a single base change can then be

discriminated from the target allele using a primer extension reaction with product resolution according to the mass. The results of spectra were analyzed using QGEAnalyzer software (Sequenom). When the peak areas of the target allele and competitive template allele were equal, the concentrations of the two molecules were at a 1:1 ratio, representing the amount of target DNA in the reaction. The MassARRAY analysis is very specific, since a given primer extension product can be discerned down to a resolution of 40 Daltons. Moreover, the expression levels evaluated using the MassARRAY are directly correlated with real-time PCR expression data [25].

Eighteen target genes and two internal controls were designed into separate multiplexed assays using the MassARRAY QGE assay design software (Sequenom, CA) based on the transcript sequences found at the Ensembl genome browser (http://www.ensembl.org/Homo_sapiens/index.html). The target gene panel was comprised of growth factor receptors (*EGFR, HER2, HER3, IGF1R, FGFR*), ER-related genes (*ESR1, PGR, FOXA1, LMTK3*), PI3 K pathway genes (*PTEN, INPP4B, SRC-1, DUSP4*), T-cell regulators (*CD274*[PDL-1], *PDCD1*[PD-1],*CTLA-4*), and oncogenes (*BCL-2, CCND1*[cyclinD1]). The primers for the gene expression analysis are listed in Table 1. Of the 18 genes, *PDCD1* was undetectable in more than half of the samples, and was filtered out in subsequent analysis. The internal control genes used for normalization were GAPDH and β2-microglobulin. The normalization factor was calculated for each sample using the GEOMEAN function according to the validated algorithm [26], then every expression value was corrected by its sample-specific correction factor. The final gene expression levels were dichotomized according to the median values.

Mutation detection by the MassARRAY system

We analyzed 25 somatic mutations in *PIK3CA, PIK3R1, AKT1, HER2, GATA3,* and *HER2* from 10 ng of DNA in 75 samples using the iPLEX Pro genotyping assay (Sequenom). These mutations were selected from public databases including the NCI somatic mutation data base (http://tcga-data.nci.nih.gov/docs/somatic_mutations/tcga_mutations.htm) and COSMIC (http://www.sanger.ac.uk/genetics/CGP/cosmic/). The iPLEX assay involves a three-step process composed of a multiplexed PCR step to amplify a 100–150-bp fragment spanning the mutation of interest, then removes unincorporated primers and deoxyribonucleotide triphosphates (dNTPs) using ExoSAP available as part of the iPLEX Pro kit, followed by a single-base primer extension assay using the iPLEX Pro Taq. The extension primers were designed for the region immediately adjacent to the mutation site and were extended by a single nucleotide at the mutation site, dependent on the template sequence [wild type or mutant]. The allelic-specific difference in mass between the extended products, was measured using MALDI-TOF. The data analysis was performed using MassArray Typer Analyzer software 4.0.4.22 (Sequenom), which compares the peaks of the wild type and all suspected mutations. Reactions with >10 % of the detected mass corresponding to the mutated allele were regarded as being positive for mutations. Then a mutation report was generated detailing the specific mutations and the ratios of wild type and mutation peaks with the corresponding confidence levels. When a mutation was detected with a low confidence, the spectra were visually checked and abnormal peak was removed from the mutation report manually. Multiplexed assays were designed using the Assay Design Sequenom software. The PCR primers and extension primers for the various mutations are described in Supplementary Table 2.

Immunohistochemical (IHC) analysis

An HER2-overexpression status was defined as a 3+ staining intensity, that is, more than 10 % of the cancer cells were markedly positive according to IHC using the DAKO HerceptTest (DAKO, Glostrup, Denmark) or as the presence of *HER2* gene amplification, that is, a HER2/CEP17 signal ratio of 2.0 according to the fluorescent in situ hybridization (PathVysion FISH; Abbott, Abbott Park, IL).

Biomarker expression based on the IHC assays was scored by two pathologists (T.S for ER, PTEN, and BCL-2 and K.K for cyclin D1), who were unaware of the patients' clinical data. Immunostaining for ER and cyclin D1 was performed on a Ventana Autostainer (Ventana Medical Systems, Tuscon, AZ) using standard laboratory protocols. Briefly, the slides were dried at 60 °C for 1 h and deparaffinized using EZ Prep (Ventana Medical Systems) at 75 °C for 4 min. The cells were conditioned (heat pretreatment) using a CC1 solution containing Tris/borate/ethylenediaminetetraacetic acid at 100 °C for 60 min. Endogenous peroxidase was blocked with 1 % hydrogen peroxidase (H2O2) at 37 °C for 4 min. The antibody for ER (Ventana, SP1, diluted solution) or Cyclin D1 (Nichirei, SP4, 1:2) was incubated at 37 °C for 32 min. Antibody incubation for Cyclin D1 was followed by 8 min incubation with Amplifier A (Ventana) and 8 min incubation with Amplifier B (Ventana). Blocker A and B (Ventana) were added for 4 min, respectively. Signals were detected using an i-view DAB detection kit (Ventana Medical Systems) based on the labeled streptavidin–biotin method. The protocol for using the kit included treatment with biotinylated immunoglobulin (8 min), streptavidin-horseradish peroxidase (8 min), diaminobenzedine (chromogen + substrate) (8 min), and copper (4 min) at 37 °C. Immunostaining for PTEN and Bcl-2 was detected using

Table 1 PCR (F, forward; R, reverse) and extension (EXT) primers for quantitative gene expression analysis

Gene	F primer	R primer	EXT Primer
EGFR	ACGTTGGATGGTATGCACTCAGAGTTCTCC	ACGTTGGATGAGGGAATGCGTGGACAAGTG	CTTGGCTCACCCTCCAG
DUSP4	ACGTTGGATGCGACATCTGCCTGCTCAAAG	ACGTTGGATGGGGCCTTGGTTTTAGAACAG	CTGCTCAAAGGCGGCTA
FGFR1	ACGTTGGATGCATCAACCACACATACCAGC	ACGTTGGATGTGTTTTGTTGGCGGGCAACC	TGGATGTCGTGGAGCGG
LMTK3	ACGTTGGATGAGATGGGTTTCCCAGCAACG	ACGTTGGATGGGAAATCCTCCGCCCACTC	TACAGCGGCTTTGGAGGC
IGF1R	ACGTTGGATGAGTCGTTGCGGATGTCGATG	ACGTTGGATGTCCTGTTTCTCTCCGCCGC	CCGGCCCGCAGATTTCTCC
INPP4B	ACGTTGGATGAGACATCGTCTTCAGCCAAG	ACGTTGGATGGCCTGGGTCATACAGACTTG	TCAGCCAAGCACTTGCTGG
PDCD1	ACGTTGGATGTTCGGTCACCACGAGCAGG	ACGTTGGATGTGCTACAACTGGGCTGGCG	GGTGTCTGGGGAGTCTAAG
CTLA	ACGTTGGATGTTTCTCCTCACAGCTGTTTC	ACGTTGGATGGGCATTTTCACATAGACCCC	TTTGAGCAAAATGCTAAAGA
PGR	ACGTTGGATGGAGCTCACAGCGTTTCTATC	ACGTTGGATGTTCAAGCAGTACAGATGAAG	GATAACTTGCATGATCTTGTC
CCND1	ACGTTGGATGTGCATCTACACCGACAACTC	ACGTTGGATGTCCACTTGAGCTTGTTCACC	TAGAGGAGCTGCTGCAAATGG
NCPOA1	ACGTTGGATGATCTTGAGGAGAAAGCCCAC	ACGTTGGATGCAAAGTCCAGACATGCAACC	CAGCCCACTGTGCTCCCTGTCG
PTEN	ACGTTGGATGAAAGACATTATGACACCGCC	ACGTTGGATGTCTAGCTGTGGTGGGTTATG	GAATTTAATTGCAGAGTTGCAC
GAPDH	ACGTTGGATGTTAAAAGCAGCCCTGGTGAC	ACGTTGGATGCACATCGCTCAGACACCATG	ACAATACGACCAAATCCGTTGAC
ERBB3	ACGTTGGATGTCATGGGCAAATTCTCGAGG	ACGTTGGATGCGAAATTATAGCCGAGGAGG	TCAAATTCTCGAGGCTCCCCATTC
ESR1	ACGTTGGATGAGGGAGAGGAGTTTGTGTGC	ACGTTGGATGCCTTCTCTTCCAGAGACTTC	CTTATTTTGCTTAATTCTGGAGTG
B2M	ACGTTGGATGCGAGACATGTAAGCAGCATC	ACGTTGGATGAGCAAGCAAGCAGAATTTGG	GTAAGCAGCATCATGGAGGTTTGA
BCL2	ACGTTGGATGTACAGTTCCACAAAGGCATC	ACGTTGGATGGGATGACTGAGTACCTGAAC	AAAGTTCCACAAAGGCATCCCAGCC
ERBB2	ACGTTGGATGACAGCTGGTGGCAGGCCAGG	ACGTTGGATGACCAAGCTCTGCTCCACACT	CGGCCAGGCCCTCGCCCACACACTCG
FOXA1	ACGTTGGATGATGAAACCAGCGACTGGAAC	ACGTTGGATGTGAGTTCATGTTGCTGACCG	ACTACGCAGACACGCAGGAGGCCTAC
CD274	ACGTTGGATGGTTTGTATCTTGGATGCCAC	ACGTTGGATGTATGCCTTGGTGTAGCACTG	GTTTCACATCCATCATTCTCCCTTTTC

Table 2 PCR (F, forward; R, reverse) and extension (EXT) primers for mutations analysis

Well	Gene	Expected aminoacid substitutions	F primer	R primer	EXT Primer
W1	*PIK3CA*	*E542 K*	ACGTTGGATGGCAATTTCTACACGAGATCC	ACGTTGGATGTAGCACTTACCTGTGACTCC	CACGAGATCCTCTCTCT
W1	*AKT1*	*E17 K*	ACGTTGGATGTCTGACGGGTAGAGTGTGC	ACGTTGGATGTTCTTGAGGAGGAAGTAGCG	CCCGCACGTCTGTAGGG
W1	*HER2*	*V842I*	ACGTTGGATGTACATGGGTGCTTCCCATTC	ACGTTGGATGGACTCTTGACCAGCACGTTC	TGGAGGATGTGCGGCTC
W1	*PIK3CA*	*H1047Y*	ACGTTGGATGCATTTTTGTTGTCCAGCCAC	ACGTTGGATGTCGAAAGACCCTAGCCTTAG	GTTGTCCAGCCACCATGAT
W1	*PIK3CA*	*Q546R*	ACGTTGGATGTAGCACTTACCTGTGACTCC	ACGTTGGATGGCAATTTCTACACGAGATCC	CTCCATAGAAAATCTTTCTCC
W1	*PIK3CA*	*C420R*	ACGTTGGATGCCTTTTGGGGAAGAAAAGTG	ACGTTGGATGAGTTTATATTTCCCCATGCC	TTCTTTGTTTTTTAAGGAACAC
W1	*PIK3R1*	*N345 K*	ACGTTGGATGGGGTTATAAATAGTGCACTC	ACGTTGGATGGCATCAGCATTTGACTTTACC	AATTCTTTGTGCAACCTACGTGAA
W1	*HER2*	*D769H/Y*	ACGTTGGATGTGAAAATTCCAGTGGCCATC	ACGTTGGATGTCCTTCCTGTCCTCCTAGC	CCCCCAAAGCCAACAAAGAAATCTTA
W2	*GATA3*	*G315delGGinsAGC*	ACGTTGGATGTCTCTCCCCACTCTCAGTCT	ACGTTGGATGTTGTGGTGGTCTGACAGTTC	TGCAGCCAGGAGAGCAG
W2	*PIK3CA*	*E545 K*	ACGTTGGATGTACACGAGATCCTCTCTCTG	ACGTTGGATGTAGCACTTACCTGTGACTCC	CCTCTCTCTGAAATCACT
W2	*HER2*	*V777L*	ACGTTGGATGTTGTCCCCAGGAAGCATACG	ACGTTGGATGAGAAGGCGGGAGACATATGG	AGCATACGTGATGGCTGGT
W2	*GATA3*	*R331delAGG R331insTGGAGGA*	ACGTTGGATGAACTGTCAGACCACCACAAC	ACGTTGGATGTGAAGCTTGTAGTAGAGCCC	CACAACCACACTCTGGAGGA
W2	*PIK3CA*	*D440G*	ACGTTGGATGTGGGATGTGCGGGTATATTC	ACGTTGGATGCTTTCTAGGATCAAGTTGTC	TTTCCCTACAGCTTCAATATTA
W2	*HER2*	*S310F*	ACGTTGGATGCTGTCACCTCTTGGTTGTGC	ACGTTGGATGAGACAACTACCTTTCTACGG	GCAGGGGGCAGACGAGGGTGCAG
W2	*GATA3*	*P409insG*	ACGTTGGATGTCAGCATGTGGCTGGAGTG	ACGTTGGATGAGAACAGCTCGTTTAACCCG	CATGTGGCTGGAGTGGCTGAAGGGC
W3	*GATA3*	*R399delGA*	ACGTTGGATGAGAACAGCTCGTTTAACCCG	ACGTTGGATGTCAGCATGTGGCTGGAGTG	CCCGGCCGCCCTCTCCA
W3	*HER2*	*L755S*	ACGTTGGATGTGAAAATTCCAGTGGCCATC	ACGTTGGATGTCCTTCCTGTCCTCCTAGC	CAGTGGCCATCAAAGTGT
W3	*PIK3CA*	*E545A/G*	ACGTTGGATGTACACGAGATCCTCTCTCTG	ACGTTGGATGTAGCACTTACCTGTGACTCC	CCTCTCTCTGAAATCACTG
W3	*HER2*	*G309A/E*	ACGTTGGATGAGACAACTACCTTTCTACGG	ACGTTGGATGCTGTCACCTCTTGGTTGTGC	CTACCTTTCTACGGACGTGG
W3	*PIK3CA*	*H1047R/L*	ACGTTGGATGTCCATTTTTGTTGTCCAGCC	ACGTTGGATGTCGAAAGACCCTAGCCTTAG	TTTTGTTGTCCAGCCACCATGA

the EnVision™+system (DAKO, Copenhagen, Denmark). Formalin-fixed, paraffin-embedded sections were deparaffinized in xylene and rehydrated in a series of graded concentrations of ethanols. Heat-induced epitope retrieval using Target Retrieval Solution, pH9 (DAKO, Copenhagen, Denmark) was performed at 98 °C for 30 min and then cooled at room temperature for 20 min. Endogenous peroxidase was blocked in 3 % hydrogen peroxide in water for 5 min. The sections were then rinsed with TBS-Tween20 (TBS containing 0.1 % Tween20), treated with protein block (DAKO, Copenhagen, Denmark) for 10 min to block nonspecific background staining, and incubated with mouse monoclonal antibodies against PTEN (DAKO, clone 6H2.1, 1:100) or Bcl-2 (DAKO, clone 124, 1:200) overnight at 4 °C. The sections were rinsed with TBS-Tween20 and incubated with secondary goat anti-mouse antibody (DAKO, HRP labeled polymer) at room temperature for 30 min. The color reaction was developed using 3,3′-diaminobenzidine for 5 min. The sections were then counterstained with Meyer's hematoxylin and mounted.

Only nuclear staining was considered to be specific in IHC for ER and cyclin D1. ER was classified as positive if more than 1 % of the cancer cell nuclei were stained regardless of the staining intensity and was scored as follows: 0, 0 %,; 1, 1–9 %; 2, 10–49 %; or 3, ≥50 %. These criteria were modified from the J-score, which provide results that are very similar to Allred score [27]. Cyclin D1 was scored by staining intensity (0, negative; 1, weak; 2, moderate; and 3, strong staining) and the percentage of positive cells (0, none; 1, <1 %; 2, 1–10 %; 3, 10–33 %; 4, 33–67 % and 5, >67 %.) according to a previous report [28]. The proportion and intensity scores were then added to obtain a total score, which ranged from 0 to 8. The tumors were then categorized into three groups: negative/weak expression (total score, 0–2), intermediate expression (total score, 3–5), and strong expression (total score, 6–8).

PTEN and BCL-2 staining were located mainly in the cytoplasm and were scored semiquantitatively on staining intensity (0, negative; 1, weak; 2, moderate; and 3, strong staining) and percentage of positive cells (0, <1 %; 1, 1–10 %; 2, 11–50 %; 3, 51–80 %; and 4, ≥80 %) according to the previous reports [29, 30]. The PTEN or BCL-2 IHC score was calculated as (staining intensity) × (percentage of positive cells). PTEN loss was defined as an IHC score of 3 or less [30, 31]. The BCL-2 expression scores were categorized into four groups: negative (score of 0–2), weak (score of 3–4) intermediate (score of 6–8), and strong expression (score of 9–12).

Statistical methods

The Spearman rank correlation analysis was used to assess the correlation between the transcriptional expression levels of *CCND1* and other genes, which were treated as continuous variable. The *P* value indicates the level of significance. An analysis of predictors of pCR among gene expression, mutation, and clinicopathological parameters stratified according to the ER protein status was performed using logistic regression analysis. Excluding genes whose expressions were highly correlated with *CCND1*, variables with *P* values of ≤ 0.05 in univariate analysis of patients with ER-positive tumors were included in the multivariate analysis. All the statistical analyses were performed using IBM SPSS Statistics 20 (Armonk, NY, USA).

Table 3 Patient characteristics

Characteristics	All $n = 75$ (%)	ER-negative $n = 40$ (%)	ER-positive $n = 35$ (%)
Median age, years	58 (26–71)	58 (40–69)	58 (26–71)
Histology			
Invasive ductal carcinoma	73 (97)	39 (97)	34 (97)
Apocrine carcinoma	2 (3)	1 (3)	1 (3)
Primary tumor			
T1–2	59 (79)	27 (67)	32 (91)
T3–4	16 (21)	13 (33)	3 (9)
Axillary node			
N0	13 (17)	6 (15)	7 (20)
N1–3	62 (83)	34 (85)	28 (80)
Stage			
I	2 (3)	0 (0)	2 (6)
II	43 (57)	20 (50)	23 (66)
III	30 (40)	20 (50)	10 (29)
PgR IHC positive	12 (16)	0 (0)	12 (34)
Neoadjuvant regimens			
FEC and PTX with trastuzumab	68 (91)	37 (93)	31 (89)
FEC and DTX with trastuzumab	7 (9)	3 (8)	4 (11)
pCR (ypT0/is ypN0)	39 (52)	25 (63)	14 (40)

HR hormonal receptor, *ER* estrogen receptor, *PgR* progesterone receptor, *FEC, 5-FU* epirubicin and cyclophosphamide, *PTX* paclitaxel, *DTX* docetaxel, *pCR* pathological complete response

Results

The patient characteristics are shown in Table 3. Almost all the patients had stage II or III disease. Forty-seven percent of the patients had HER2-positive/ER-positive tumors. The pCR rates were 52 % for all 75 patients, and 40 % for in the ER-positive patients; this latter value was significantly lower than the value of 63 % observed for ER-negative patients ($P = 0.054$, odds ratio [OR] 0.40 [95 % CI 0.16–1.02]).

Gene expression analysis and correlation with IHC protein expressions

In an expression analysis of 1,275 genes (17 genes, 75 samples), 1,245 (97.6 %) were successfully analyzed. For the HER2-positive/ER-positive tumors, the median *CCND1* and *BCL-2* levels (3,540 and 141 molecules) were 2.1 and 2.2 times higher than those for the HER2-positive/ER-negative patients (1,714 and 63.0 molecules), respectively. Representative staining patterns of PTEN, cyclin D1, and BCL-2 protein expression are shown in Fig. 1.

The transcriptional mRNA expression of *ESR1* ranged from 5.6 to 9,405.0 (median, 95.0) and was highly correlated with the IHC classification of ER protein expression (Spearman's *rho* = 0.78; $P < 0.001$). Figure 2a shows the *ESR1* mRNA levels in different IHC scoring groups. The correlation between ESR1 gene expression (> median) and pCR was marginally significant ($P = 0.062$; OR 0.41 [95 % CI 0.16–1.05]), which was very similar to that of ER protein expression.

The correlations between the gene and protein expression levels of cyclin D1 or BCL-2 were also significant (Spearman's *rho* = 0.53; $P < 0.001$ or 0.50; $P < 0.001$, respectively) and are shown according to the IHC scores in Fig. 2b, c, respectively. In the PTEN IHC analysis, 12 tumors (16 %) were classified as exhibiting PTEN loss.

Mutation analysis

The overall incidence of PIK3CA mutations was 33 % (25 tumors), with 25 % (19 tumors) occurring at the three hotspot sites of E545 K, E542 K, and H1047R and 8 % (6 tumors) consisting of rare mutations (H1047L, N345 K and C420R). No difference was identified in the PIK3CA mutation rate between ER-positive tumors (13/35, 37 %) and ER–negative tumors (12/40, 30 %). Only one mutation at HER2 (V842I) was found in a patient with an ER-positive tumor; this patient did not achieve a pCR and relapsed and died at 7 and 41 months after diagnosis, respectively. GATA3 (R331delAGG) was found in one patient with an ER-positive tumor who achieved a pCR. Because of the low mutation rate, the predictive significance of the HER2 or GATA3 mutation could not be determined. No AKT1 (E17 K) mutation was found.

Predictors of pCR based on a logistic regression analysis

We conducted separate evaluations of ER-positive and ER-negative tumors using logistic regression analysis (Table 4). In the HER2-positive/ER-positive tumors, a pCR was associated with high mRNA levels of *ESR1, PGR, LMTK3, HER2, IGF1R, INPP4B, CTLA4, PDL-1, BCL-2, and CCND1*. In contrast, none of these genes were significantly correlated with a pCR in the HER2-positive/ER-negative tumors and only *EGFR* was significantly correlated with a pCR. PIK3A mutations or PTEN loss as determined using IHC were not associated with a pCR in either group.

In the HER2-positive/ER-positive tumors, a Spearman rank correlation analysis was used to assess the correlation between the transcriptional expression levels of *CCND1* and other genes, which were regarded as continuous variables (Table 5). *CCND1* gene expression was significantly correlated with *ESR1* ($r = 0.58$), *PGR* ($r = 0.64$), and *IGF1R* ($r = 0.59$); thus, *PDL-1, CTLA4, HER2, INPP4B, BCL-2*, and *CCND1* were tested in the multivariate model. *CCND1* [$P = 0.043$; OR, 0.16 (0.03–0.94)] and *HER2* [$P = 0.012$; OR, 11.2 (1.7–73.7)] retained a predictive value for pCR (Table 6).

Discussion

Recently, Denkert et al. [32] demonstrated that *HER2* mRNA expression in a neoadjuvant setting was associated with a pCR in patients with HER2-positive/ESR1-positive tumors, but not in those with HER2-positive/ESR1-negative tumors. Our data also showed similar results, with an association between *HER2* mRNA expression and a pCR in the ER-positive tumors, but not in ER-negative tumors (Table 5). In addition, the expression of *ESR1* mRNA and the IHC classification for ER were strongly correlated in our study, consistent with the results of a previous study [33]. Similarly, the gene and protein expressions of cyclin D1 and BCL-2 were also correlated. These findings support the reliability of the gene expression data analyzed using the MassARRAY system.

Our investigation implies that a high level of *CCND1* mRNA expression, independent of *HER2* mRNA, predicts a poor response to neoadjuvant treatment with trastuzumab plus anthracyline-taxane chemotherapy in patients with HER2-positive/ER-positive tumors. In contrast, this phenomenon was not observed in the ER-negative subset with only *EGFR* mRNA expression predicting a pCR. Furthermore, considerable differences in gene expression were observed between ER-positive/HER2-positive and ER-negative/HER2-positive tumors in the presently reported neoadjuvant setting. Indeed, pertuzuamb, trastuzumab-emtansine, PI3K inhibitors, and mTOR inhibitors may combat chemotherapy resistance driven by HER2/HER3-PIK3-mTOR pathway alterations, but whether these new drugs can combat the resistance driven by ER in HER2-positive tumors remains unclear. Therefore, further studies are needed to categorize the different treatment strategies stratified according to ER status.

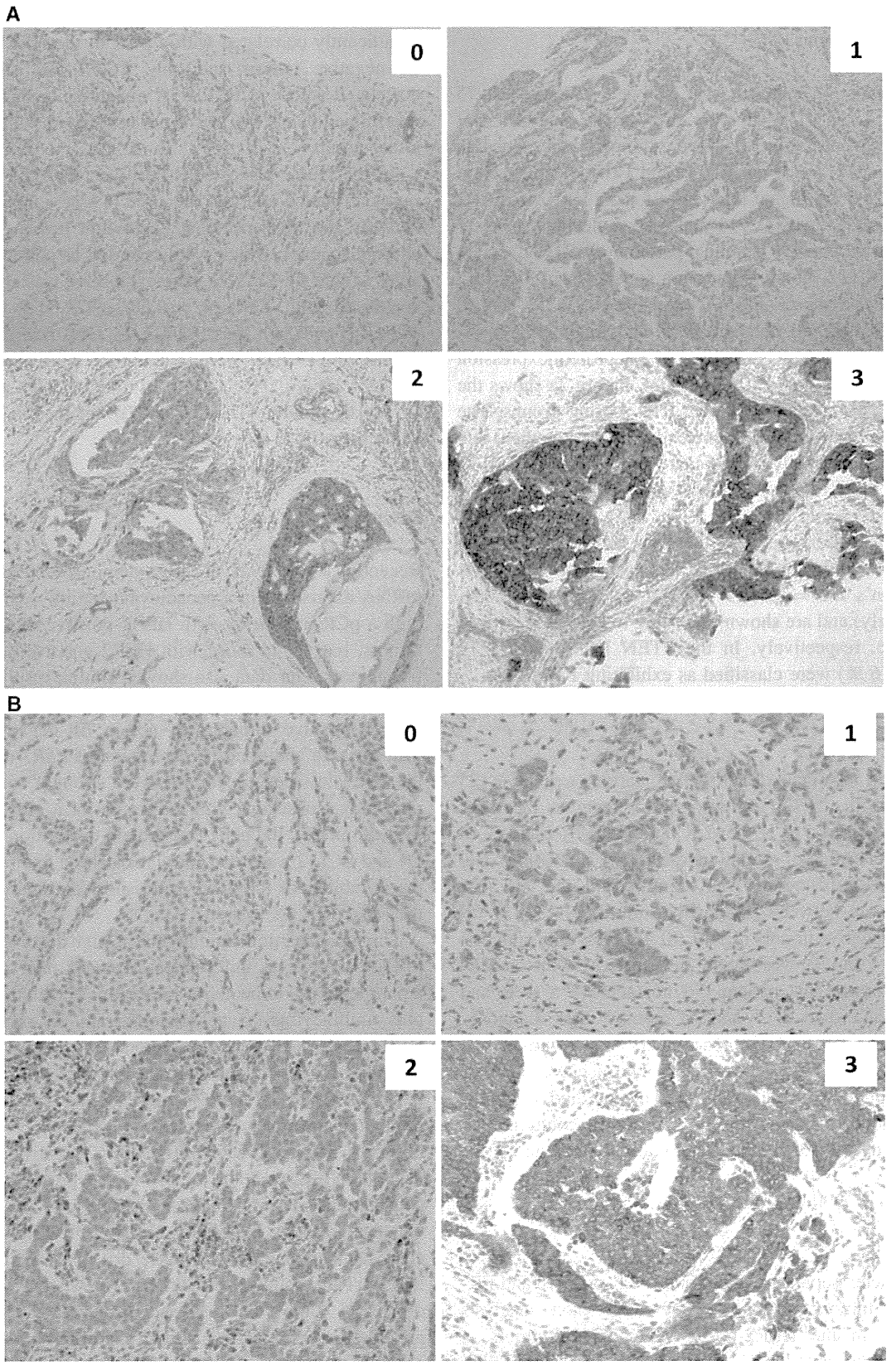
A
0
1
2
3
B
0
1
2
3

◀**Fig. 1** Correlation of protein and mRNA expression. Column scatter graphs were prepared with GraphPad Prism 5 to show the mRNA levels in different IHC scoring groups. The horizontal line in each column represents the median transcription value for the specific IHC score group. **a** ER protein and ESR1 mRNA levels; Spearman's *rho* = 0.78; $P < 0.001$). **b** cyclin D1 protein and mRNA levels; Spearman's *rho* = 0.53; $P < 0.001$ **c** BCL-2 protein and mRNA levels; Spearman's *rho* = 0.50; $P < 0.001$

Cyclin D1 binds to CDK4/6 [21, 22] and activates CDK4 [23]. Preclinical studies identified the ER subtype, the elevated expression of cyclin D1 and Rb protein, and a reduction in p16 expression as being associated with sensitivity to PD 0332991 (palbociclib) [34]. Therefore, cyclin D1 could be a potential molecular biomarker of CDK4/6 inhibitors including palbociclib, which is development for the treatment of ER-positive metastatic breast cancer patients. Although this population has HER2-negative tumors, our investigation showed that the median *CCND1* gene expression levels in HER2-positive/ER-positive tumors were 2.1 times higher than in HER2-positive/ER-negative tumors. Palbociclib was synergistic with tamoxifen and trastuzumab in ER-positive and HER2-amplified cell lines [34]. Based on these evidences, palbociclib might be effective even in HER2-positive/ER-positive breast cancer.

Finn et al. reported the final results of a randomized phase II trial examining the use of palbociclib, a CDK4/6 inhibitor, in ER-positive HER2-negative breast cancer patients [35]. The participants were divided into two parts: an unselected population (Part 1) and patients with *CCND1* amplification and/or the loss of p16 (Part 2). The hazard ratio was much better in Part 1(0.299) than in Part 2 (0.508). Therefore, *CCND1* amplification is not presently regarded as a biomarker of palbociclib. Given that CDK4/6 inhibition was shown to be effective, *CCND1* amplification may be just one of several activators of CDK4/6. In breast cancer, cyclin D1 is overexpressed in 50 % of breast cancer specimens, while the corresponding *CCND1* gene is amplified in only 15 % [20]; thus, cyclin D1 is overexpressed in the absence of *CCND1* amplification in 35 % of breast cancer patients. Therefore, we hypothesized that the overexpression of *CCND1* mRNA may explain CDK4/6 activation better than *CCND1* amplification.

The TCGA breast cancer study showed low levels (less than 1 %) of RB1 mutations in luminal and HER2 enriched subtypes of breast cancer [36]. In addition, the RB gene

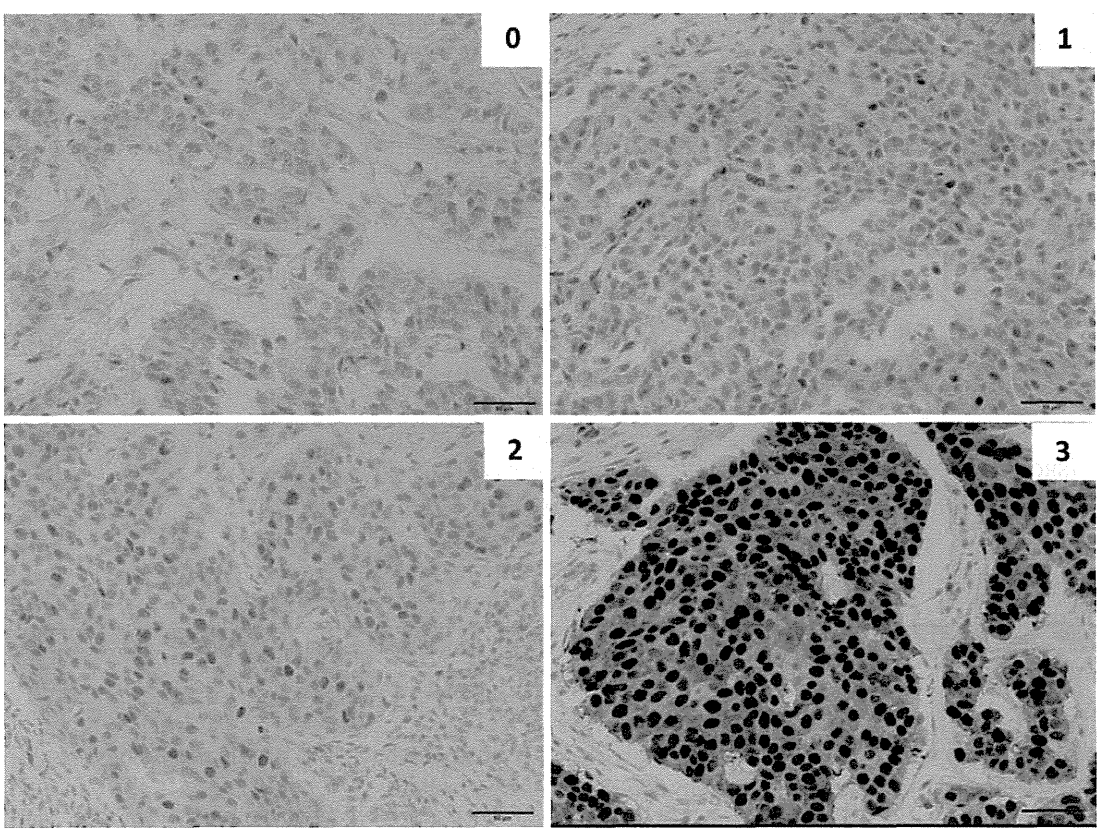

Fig. 1 continued

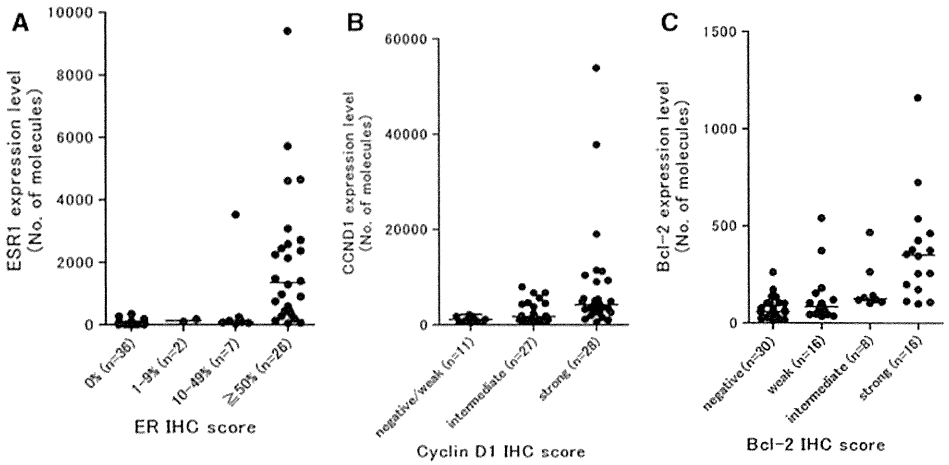

Fig. 2 Representative staining intensity of PTEN, BCL-2, and cyclin D1. Immunohistochemical staining intensity of **a** PTEN, **b** BCL-2, and **c** cyclin D1 was scored semiquantitatively; 0, negative; 1, weak; 2, moderate; and 3, strong staining

Table 4 Univariate analysis on predictors of pCR when stratified with ER status

	ER-negative (n = 40)		ER-positive (n = 35)	
	P value	OR (95 % CI)	P value	OR (95 % CI)
Age ≥ 50 years	0.46	1.52 (0.50–4.64)	0.45	1.83 (0.38–8.78)
T3–4	0.75	0.86 (0.35–2.15)	0.51	1.70 (0.35–8.34)
N1–3	0.90	0.94 (0.38–2.33)	0.31	0.42 (0.08–2.25)
Stage III	0.97	0.98 (0.39–2.49)	1.00	1.00 (0.22–4.47)
PI3 K path alteration	0.12	2.98 (0.74–11.9)	0.22	0.42 (0.10–1.68)
mRNA expression level (>median)				
ESR1	0.84	0.88 (0.24–3.26)	0.006	0.11 (0.02–0.54)
PgR	0.17	0.37 (0.09–1.52)	0.003	0.07 (0.01–0.39)
FOXA1	0.74	1.24 (0.34–4.46)	0.13	0.34 (0.08–1.39)
LMTK3	1.0	1.00 (0.26–3.82)	0.032	0.20 (0.05–0.87)
DUSP4	0.33	1.91 (0.52–7.01)	0.58	1.47 (0.38–5.72)
HER2	0.74	0.81 (0.22–2.91)	0.003	15.0 (2.55–88.2)
HER3	0.74	1.24 (0.34–4.46)	0.41	0.56 (0.14–2.21)
EGFR	0.035	0.22 (0.05–0.90)	0.22	0.42 (0.10–1.68)
FGFR1	0.33	1.91 (0.52–7.01)	0.41	0.56 (0.14–2.21)
IGF1R	0.74	0.81 (0.22–2.91)	0.006	0.11 (0.02–0.54)
PTEN	0.74	1.24 (0.34–4.46)	0.22	2.40 (0.60–9.67)
INPP4B	0.33	0.52 (0.14–1.92)	0.013	0.14 (0.03–0.65)
NCPOA1 (SRC1)	0.74	0.81 (0.22–2.91)	0.89	0.91 (0.24–3.52)
CD274 (PDL1)	0.63	1.40 (0.35–5.54)	0.032	5.00 (1.15–21.8)
CTLA4	0.50	1.58 (0.42–5.95)	0.22	2.40 (0.60–9.67)
BCL-2	0.39	0.56 (0.14–2.10)	0.006	0.11 (0.02–0.54)
CCND1 (cyclin D1)	0.74	0.81 (0.22–2.91)	0.006	0.11 (0.02–0.54)

PI3 K path alteration, PIK3CA mutation and/or immunohistochemical PTEN loss; CI, confidence interval; pCR, pathologic complete response (ypT0/is ypN0)

expression signature is reportedly associated with the response to chemotherapy or endocrine therapy [37–39]. However, the significance of RB mutations in our sample set of 75 patients was difficult to determine because of the low frequency. We think that the significance of *CCND1* overexpression and RB1 mutations should be clarified in a larger cohort.

HER3, *EGFR*, *FGFR1*, *SRC1*, *FOXA1*, and PIK3CA mutation and/or PTEN loss were not significantly predictive of pCR among HER2-positive/ER-positive tumors.

Table 5 Spearman's correlation analysis with *CCND1* mRNA expression (continuous variable)

	ER-negative ($n = 40$)		ER-positive ($n = 35$)	
	P	Spearman's rho	*P*	Spearman's rho
IHC cyclin D1	0.88	0.03	<0.001	0.53
IHC ER	–	–	0.50	0.12
PI3K path alteration	0.82	0.03	0.42	−0.14
mRNA expression level (continuous variable)				
ESR1	0.85	−0.03	<0.001	0.58
PGR	0.006	−0.47	<0.001	0.64
FOXA1	0.13	0.24	0.55	0.67
LMTK3	0.63	−0.08	0.027	0.37
DUSP4	0.007	0.42	0.92	−0.02
HER2	0.52	−0.11	0.041	−0.35
HER3	0.005	−0.44	0.039	0.35
EGFR	0.16	−0.23	0.72	−0.07
FGFR1	0.02	0.37	<0.001	0.56
IGF1R	<0.001	0.67	<0.001	0.59
PTEN	0.001	0.50	0.19	0.23
INPP4B	0.33	0.23	0.002	0.50
NCPOA1 (SRC1)	0.02	0.36	0.68	0.07
CD274 (PDL1)	0.89	−0.02	0.09	−0.30
CTLA4	0.94	−0.01	0.10	0.28
BCL-2	0.38	0.15	<0.001	0.40

PI3K path alteration, PIK3CA mutation and/or immunohistochemical PTEN loss; CI, confidence interval

One possible explanation is that their influence on resistance to neoadjuvant chemotherapy might be so small that it was difficult to detect in our small subset. DUSP4 might be an important regulator of mitogen-activated protein kinase (MAPK) pathway in triple-negative breast cancer, but might not be as an important in HER2-positive breast cancer. Similarly, CTLA4 might be important in melanoma, but not in HER2-positive breast cancer.

In HER2-positive/ER-negative tumors, only *EGFR* was significantly correlated with a pCR. The significance of EGFR protein expression is controversial in HER2-postive breast cancer. The benefit of lapatinib, an EGFR and HER2 dual inhibitor, was greater in patients with HER2-amplified, ER-negative tumors; however, its benefit was not correlated with EGFR expression [40]. On the other hand, a high EGFR expression was associated with a decreased benefit from trastuzumab in the N9831 trial, which assessed the efficacy of adding 52 weeks of trastuzumab to the standard chemotherapy [41]. The EGFR pathway is a complex signaling network, and EGFR-associated prognostic signatures were highly expressed in HER2-positive/ER-negative tumors [42].

Table 6 Multivariate analysis on predictors of pCR in patients with HER2-positive ER-positive breast cancer

$n = 35$	*P* value	Odds ratio (95 % CI)
mRNA expression level (>median)		
HER2	0.012	11.2 (1.7–73.7)
CCND1 (cyclin D1)	0.043	0.16 (0.03–0.94)

Variables tested for inclusion in the multivariate logistic regression model were *HER2, CCND1, INPP4B, BCL-2, LMTK3,* and *PDL1*. CI, confidence interval

Therefore, the significance of EGFR should be confirmed in this subset using an EGFR-associated gene expression signature.

The main limitation of our study was its retrospective nature and the lack of an analysis of samples in a validation set. However, the advantages of this study were that a nearly identical NAC comprised anthracycline, taxane, and trastuzumab in all the patients, and a precise evaluation of the gene expression levels using by MassARRAY, the results of which were directly correlated with real-time PCR expression data and significantly correlated with the corresponding protein expression levels. In conclusion, our results provide evidence that a high level of *CCND1* gene expression is an independent predictor of a poor response to NAC resistance in addition to provide a rationale for the evaluation of CDK4/6 inhibitors in HER2-positive/ER-positive breast cancer.

Conflict of interest Dr. Hironobu Minami has received an unrestricted research grant and honoraria for his activities as a speaker and a member of the committee for clinical studies from Chugai Pharmaceutical, the manufacturer of trastuzumab. The other authors have declared no conflict of interest.

Funding The study protocol was funded by research Grants from the Daiwa Securities Health Foundation.

References

1. von Minckwitz G, Untch M, Blohmer JU, Costa SD, Eidtmann H, Fasching PA, Gerber B, Eiermann W, Hilfrich J, Huober J, Jackisch C, Kaufmann M, Konecny GE, Denkert C, Nekljudova V, Mehta K, Loibl S (2012) Definition and impact of pathologic complete response on prognosis after neoadjuvant chemotherapy in various intrinsic breast cancer subtypes. J Clin Oncol 30(15):1796–1804. doi:10.1200/JCO.2011.38.8595
2. Cortazar P, Zhang L, Untch M, Mehta K, Costantino JP, Wolmark N, Bonnefoi H, Cameron D, Gianni L, Valagussa P, Swain SM, Prowell T, Loibl S, Wickerham DL, Bogaerts J, Baselga J, Perou C, Blumenthal G, Blohmer J, Mamounas EP, Bergh J, Semiglazov V, Justice R, Eidtmann H, Paik S, Piccart M, Sridhara R, Fasching PA, Slaets L, Tang S, Gerber B, Geyer CE, Jr., Pazdur R, Ditsch N, Rastogi P, Eiermann W, von Minckwitz G

(2014) Pathological complete response and long-term clinical benefit in breast cancer: the CTNeoBC pooled analysis. Lancet:Epub 18/Feb/2014. doi:10.1016/S0140-6736(13)62422-8
3. Robidoux A, Tang G, Rastogi P, Geyer CE Jr, Azar CA, Atkins JN, Fehrenbacher L, Bear HD, Baez-Diaz L, Sarwar S, Margolese RG, Farrar WB, Brufsky AM, Shibata HR, Bandos H, Paik S, Costantino JP, Swain SM, Mamounas EP, Wolmark N (2013) Lapatinib as a component of neoadjuvant therapy for HER2-positive operable breast cancer (NSABP protocol B-41): an open-label, randomised phase 3 trial. Lancet Oncol 14(12):1183–1192. doi:10.1016/S1470-2045(13)70411-X
4. Baselga J, Bradbury I, Eidtmann H, Di Cosimo S, de Azambuja E, Aura C, Gomez H, Dinh P, Fauria K, Van Dooren V, Aktan G, Goldhirsch A, Chang TW, Horvath Z, Coccia-Portugal M, Domont J, Tseng LM, Kunz G, Sohn JH, Semiglazov V, Lerzo G, Palacova M, Probachai V, Pusztai L, Untch M, Gelber RD, Piccart-Gebhart M (2012) Lapatinib with trastuzumab for HER2-positive early breast cancer (NeoALTTO): a randomised, open-label, multicentre, phase 3 trial. Lancet 379(9816):633–640. doi:10.1016/S0140-6736(11)61847-3
5. Gianni L, Pienkowski T, Im YH, Roman L, Tseng LM, Liu MC, Lluch A, Staroslawska E, de la Haba-Rodriguez J, Im SA, Pedrini JL, Poirier B, Morandi P, Semiglazov V, Srimuninnimit V, Bianchi G, Szado T, Ratnayake J, Ross G, Valagussa P (2012) Efficacy and safety of neoadjuvant pertuzumab and trastuzumab in women with locally advanced, inflammatory, or early HER2-positive breast cancer (NeoSphere): a randomised multicentre, open-label, phase 2 trial. Lancet Oncol 13(1):25–32. doi:10.1016/S1470-2045(11)70336-9
6. Rimawi MF, Mayer IA, Forero A, Nanda R, Goetz MP, Rodriguez AA, Pavlick AC, Wang T, Hilsenbeck SG, Gutierrez C, Schiff R, Osborne CK, Chang JC (2013) Multicenter phase II study of neoadjuvant lapatinib and trastuzumab with hormonal therapy and without chemotherapy in patients with human epidermal growth factor receptor 2-overexpressing breast cancer: TBCRC 006. J Clin Oncol 31(14):1726–1731. doi:10.1200/JCO.2012.44.8027
7. Miller TW, Perez-Torres M, Narasanna A, Guix M, Stal O, Perez-Tenorio G, Gonzalez-Angulo AM, Hennessy BT, Mills GB, Kennedy JP, Lindsley CW, Arteaga CL (2009) Loss of Phosphatase and Tensin homologue deleted on chromosome 10 engages ErbB3 and insulin-like growth factor-I receptor signaling to promote antiestrogen resistance in breast cancer. Cancer Res 69(10):4192–4201. doi:10.1158/0008-5472.CAN-09-0042
8. Frogne T, Benjaminsen RV, Sonne-Hansen K, Sorensen BS, Nexo E, Laenkholm AV, Rasmussen LM, Riese DJ 2nd, de Cremoux P, Stenvang J, Lykkesfeldt AE (2009) Activation of ErbB3, EGFR and Erk is essential for growth of human breast cancer cell lines with acquired resistance to fulvestrant. Breast Cancer Res Treat 114(2):263–275. doi:10.1007/s10549-008-0011-8
9. Giltnane JM, Ryden L, Cregger M, Bendahl PO, Jirstrom K, Rimm DL (2007) Quantitative measurement of epidermal growth factor receptor is a negative predictive factor for tamoxifen response in hormone receptor positive premenopausal breast cancer. J Clin Oncol 25(21):3007–3014. doi:10.1200/JCO.2006.08.9938
10. Turner N, Pearson A, Sharpe R, Lambros M, Geyer F, Lopez-Garcia MA, Natrajan R, Marchio C, Iorns E, Mackay A, Gillett C, Grigoriadis A, Tutt A, Reis-Filho JS, Ashworth A (2010) FGFR1 amplification drives endocrine therapy resistance and is a therapeutic target in breast cancer. Cancer Res 70(5):2085–2094. doi:10.1158/0008-5472.CAN-09-3746
11. Vaillant F, Merino D, Lee L, Breslin K, Pal B, Ritchie ME, Smyth GK, Christie M, Phillipson LJ, Burns CJ, Mann GB, Visvader JE, Lindeman GJ (2013) Targeting BCL-2 with the BH3 mimetic ABT-199 in estrogen receptor-positive breast cancer. Cancer Cell 24(1):120–129. doi:10.1016/j.ccr.2013.06.002
12. Berns EM, van Staveren IL, Klijn JG, Foekens JA (1998) Predictive value of SRC-1 for tamoxifen response of recurrent breast cancer. Breast Cancer Res Treat 48(1):87–92
13. Hurtado A, Holmes KA, Ross-Innes CS, Schmidt D, Carroll JS (2011) FOXA1 is a key determinant of estrogen receptor function and endocrine response. Nat Genet 43(1):27–33. doi:10.1038/ng.730
14. Giamas G, Filipovic A, Jacob J, Messier W, Zhang H, Yang D, Zhang W, Shifa BA, Photiou A, Tralau-Stewart C, Castellano L, Green AR, Coombes RC, Ellis IO, Ali S, Lenz HJ, Stebbing J (2011) Kinome screening for regulators of the estrogen receptor identifies LMTK3 as a new therapeutic target in breast cancer. Nat Med 17(6):715–719. doi:10.1038/nm.2351
15. Zwijsen RM, Wientjens E, Klompmaker R, van der Sman J, Bernards R, Michalides RJ (1997) CDK-independent activation of estrogen receptor by cyclin D1. Cell 88(3):405–415
16. Berns K, Horlings HM, Hennessy BT, Madiredjo M, Hijmans EM, Beelen K, Linn SC, Gonzalez-Angulo AM, Stemke-Hale K, Hauptmann M, Beijersbergen RL, Mills GB, van de Vijver MJ, Bernards R (2007) A functional genetic approach identifies the PI3 K pathway as a major determinant of trastuzumab resistance in breast cancer. Cancer Cell 12(4):395–402. doi:10.1016/j.ccr.2007.08.030
17. Jensen JD, Knoop A, Laenkholm AV, Grauslund M, Jensen MB, Santoni-Rugiu E, Andersson M, Ewertz M (2012) PIK3CA mutations, PTEN, and pHER2 expression and impact on outcome in HER2-positive early-stage breast cancer patients treated with adjuvant chemotherapy and trastuzumab. Ann Oncol 23(8):2034–2042. doi:10.1093/annonc/mdr546
18. Gewinner C, Wang ZC, Richardson A, Teruya-Feldstein J, Etemadmoghadam D, Bowtell D, Barretina J, Lin WM, Rameh L, Salmena L, Pandolfi PP, Cantley LC (2009) Evidence that inositol polyphosphate 4-phosphatase type II is a tumor suppressor that inhibits PI3 K signaling. Cancer Cell 16(2):115–125. doi:10.1016/j.ccr.2009.06.006
19. Balko JM, Cook RS, Vaught DB, Kuba MG, Miller TW, Bhola NE, Sanders ME, Granja-Ingram NM, Smith JJ, Meszoely IM, Salter J, Dowsett M, Stemke-Hale K, Gonzalez-Angulo AM, Mills GB, Pinto JA, Gomez HL, Arteaga CL (2012) Profiling of residual breast cancers after neoadjuvant chemotherapy identifies DUSP4 deficiency as a mechanism of drug resistance. Nat Med 18(7):1052–1059. doi:10.1038/nm.2795
20. Gillett C, Fantl V, Smith R, Fisher C, Bartek J, Dickson C, Barnes D, Peters G (1994) Amplification and overexpression of cyclin D1 in breast cancer detected by immunohistochemical staining. Cancer Res 54(7):1812–1817
21. Meyerson M, Harlow E (1994) Identification of G1 kinase activity for cdk6, a novel cyclin D partner. Mol Cell Biol 14(3):2077–2086
22. Matsushime H, Ewen ME, Strom DK, Kato JY, Hanks SK, Roussel MF, Sherr CJ (1992) Identification and properties of an atypical catalytic subunit (p34PSK-J3/cdk4) for mammalian D type G1 cyclins. Cell 71(2):323–334
23. Yu Q, Sicinska E, Geng Y, Ahnstrom M, Zagozdzon A, Kong Y, Gardner H, Kiyokawa H, Harris LN, Stal O, Sicinski P (2006) Requirement for CDK4 kinase function in breast cancer. Cancer Cell 9(1):23–32. doi:10.1016/j.ccr.2005.12.012
24. Ding C, Cantor CR (2003) A high-throughput gene expression analysis technique using competitive PCR and matrix-assisted laser desorption ionization time-of-flight MS. Proc Natl Acad Sci U S A 100(6):3059–3064
25. Elvidge GP, Price TS, Glenny L, Ragoussis J (2005) Development and evaluation of real competitive PCR for high-throughput

quantitative applications. Anal Biochem 339(2):231–241. doi:10.1016/j.ab.2005.01.040
26. Vandesompele J, De Preter K, Pattyn F, Poppe B, Van Roy N, De Paepe A, Speleman F (2002) Accurate normalization of real-time quantitative RT-PCR data by geometric averaging of multiple internal control genes. Genome Biol 3 (7):RESEARCH0034
27. Arihiro K, Umemura S, Kurosumi M, Moriya T, Oyama T, Yamashita H, Umekita Y, Komoike Y, Shimizu C, Fukushima H, Kajiwara H, Akiyama F (2007) Comparison of evaluations for hormone receptors in breast carcinoma using two manual and three automated immunohistochemical assays. Am J Clin Pathol 127(3):356–365. doi:10.1309/4D1A04NCDK96WFY7
28. Reis-Filho JS, Savage K, Lambros MB, James M, Steele D, Jones RL, Dowsett M (2006) Cyclin D1 protein overexpression and *CCND1* amplification in breast carcinomas: an immunohistochemical and chromogenic in situ hybridisation analysis. Mod Pathol 19(7):999–1009. doi:10.1038/modpathol.3800621
29. Dawson SJ, Makretsov N, Blows FM, Driver KE, Provenzano E, Le Quesne J, Baglietto L, Severi G, Giles GG, McLean CA, Callagy G, Green AR, Ellis I, Gelmon K, Turashvili G, Leung S, Aparicio S, Huntsman D, Caldas C, Pharoah P (2010) BCL2 in breast cancer: a favourable prognostic marker across molecular subtypes and independent of adjuvant therapy received. Br J Cancer 103(5):668–675. doi:10.1038/sj.bjc.6605736
30. Esteva FJ, Guo H, Zhang S, Santa-Maria C, Stone S, Lanchbury JS, Sahin AA, Hortobagyi GN, Yu D (2010) PTEN, PIK3CA, p-AKT, and p-p70S6 K status: association with trastuzumab response and survival in patients with HER2-positive metastatic breast cancer. Am J Pathol 177(4):1647–1656. doi:10.2353/ajpath.2010.090885
31. Nagata Y, Lan KH, Zhou X, Tan M, Esteva FJ, Sahin AA, Klos KS, Li P, Monia BP, Nguyen NT, Hortobagyi GN, Hung MC, Yu D (2004) PTEN activation contributes to tumor inhibition by trastuzumab, and loss of PTEN predicts trastuzumab resistance in patients. Cancer Cell 6(2):117–127
32. Denkert C, Huober J, Loibl S, Prinzler J, Kronenwett R, Darb-Esfahani S, Brase JC, Solbach C, Mehta K, Fasching PA, Sinn BV, Engels K, Reinisch M, Hansmann ML, Tesch H, von Minckwitz G, Untch M (2013) HER2 and ESR1 mRNA expression levels and response to neoadjuvant trastuzumab plus chemotherapy in patients with primary breast cancer. Breast Cancer Res 15(1):R11. doi:10.1186/bcr3384
33. Gong Y, Yan K, Lin F, Anderson K, Sotiriou C, Andre F, Holmes FA, Valero V, Booser D, Pippen JE Jr, Vukelja S, Gomez H, Mejia J, Barajas LJ, Hess KR, Sneige N, Hortobagyi GN, Pusztai L, Symmans WF (2007) Determination of oestrogen-receptor status and ERBB2 status of breast carcinoma: a gene-expression profiling study. Lancet Oncol 8(3):203–211. doi:10.1016/S1470-2045(07)70042-6
34. Finn RS, Dering J, Conklin D, Kalous O, Cohen DJ, Desai AJ, Ginther C, Atefi M, Chen I, Fowst C, Los G, Slamon DJ (2009) PD 0332991, a selective cyclin D kinase 4/6 inhibitor, preferentially inhibits proliferation of luminal estrogen receptor-positive human breast cancer cell lines in vitro. Breast Cancer Res 11(5):R77. doi:10.1186/bcr2419
35. Richard S, Finn JPC, Istvan Lang, Katalin Boer, Igor M. Bondarenko, Sergey O. Kulyk, Johannes Ettl, Ravindranath Patel, Tamas Pinter, Marcus Schmidt, Yaroslav V. Shparyk, Anu R. Thummala, Nataliya L. Voytko, Xin Huang, Sindy T. Kim, Sophia S. Randolph, Dennis J. Slamon Final results of a randomized Phase II study of PD 0332991, a cyclin-dependent kinase (CDK)-4/6 inhibitor, in combination with letrozole vs letrozole alone for first-line treatment of ER +/HER2- advanced breast cancer (PALOMA-1; TRIO-18) In: American Association for Cancer Research Annual Meeting, San Diego, 2014. CT101
36. TCGA (2012) Comprehensive molecular portraits of human breast tumours. Nature 490(7418):61–70. doi:10.1038/nature11412
37. Herschkowitz JI, He X, Fan C, Perou CM (2008) The functional loss of the retinoblastoma tumour suppressor is a common event in basal-like and luminal B breast carcinomas. Breast Cancer Res 10(5):R75. doi:10.1186/bcr2142
38. Witkiewicz AK, Ertel A, McFalls J, Valsecchi ME, Schwartz G, Knudsen ES (2012) RB-pathway disruption is associated with improved response to neoadjuvant chemotherapy in breast cancer. Clin Cancer Res 18(18):5110–5122. doi:10.1158/1078-0432.CCR-12-0903
39. Lehn S, Ferno M, Jirstrom K, Ryden L, Landberg G (2011) A non-functional retinoblastoma tumor suppressor (RB) pathway in premenopausal breast cancer is associated with resistance to tamoxifen. Cell Cycle 10(6):956–962
40. Finn RS, Press MF, Dering J, Arbushites M, Koehler M, Oliva C, Williams LS, Di Leo A (2009) Estrogen receptor, progesterone receptor, human epidermal growth factor receptor 2 (HER2), and epidermal growth factor receptor expression and benefit from lapatinib in a randomized trial of paclitaxel with lapatinib or placebo as first-line treatment in HER2-negative or unknown metastatic breast cancer. J Clin Oncol 27(24):3908–3915. doi:10.1200/JCO.2008.18.1925
41. Cheng H, Ballman K, Vassilakopoulou M, Dueck AC, Reinholz MM, Tenner K, Gralow J, Hudis C, Davidson NE, Fountzilas G, McCullough AE, Chen B, Psyrri A, Rimm DL, Perez EA (2014) EGFR expression is associated with decreased benefit from trastuzumab in the NCCTG N9831 (Alliance) trial. Br J Cancer. doi:10.1038/bjc.2014.442
42. Hoadley KA, Weigman VJ, Fan C, Sawyer LR, He X, Troester MA, Sartor CI, Rieger-House T, Bernard PS, Carey LA, Perou CM (2007) EGFR associated expression profiles vary with breast tumor subtype. BMC Genom 8:258. doi:10.1186/1471-2164-8-258